Supplementary Appendix

This appendix has been provided by the authors to give readers additional information about their work.

Supplement to: Tegtmeyer LC, Rust S, van Scherpenzeel M, et al. Multiple phenotypes in phosphoglucomutase 1 deficiency. N Engl J Med 2014;370:533-42. DOI: 10.1056/NEJMoa1306605

SUPPLEMENTARY APPENDIX

Contents

Responsibility for manuscript content and data evaluation 3

Supplementary Methods

Homozygosity mapping: Mapping the disease locus by linkage analysis 3
Whole exome sequencing: identification of defective PGM1 4
PCR and sequencing for mutation analysis 5
Patient cells and tissues 5
Real-time PCR for quantification of PGM1 mRNA 6
Western blotting for PGM1 6
Phosphoglucomutase 1 enzyme activity 7
Assays of transferrin glycosylation 8
Isoelectric focusing of transferrin 8
Immunoprecipitation and SDS-PAGE of transferrin 9
QTOF mass spectrometry of intact transferrin 9
Western blotting for ICAM-1 10
Assay for cellular glycosylation efficiency using modified GFP 10
Nucleotide sugar assay 10
Phosphorylated sugar assay 10
Biochemical quantification of glycogen 11
Evaluation of glycogen by electron microscopy 11
Determination of galactose kinetics in whole blood 11

Supplementary Results

Clinical phenotype 12
Sugar metabolite and glycogen quantification 13

Supplementary Discussion

Lack of effect of PGM1 deficiency on erythrocytes and the brain 14
Effect of reduced glycosylation on gonadotropin function: LH and FSH 14
Effect of reduced glycosylation on IGF1, IGFBP3, IGF-receptor and growth 15
Dilated cardiomyopathy: loss of functional interaction of PGM1 and ZASP 16

Supplementary Figures

Fig. S1 Isoelectric focusing and SDS-PAGE of transferrin 17
Fig. S2 The Beutler Test and the Modified Beutler Test 18
Fig. S3 Glycogen in hepatocytes by electron microscopy and light microscopy 19
Fig. S4 Variability of transferrin glycosylation, details by mass spectrometry 20
Fig. S5 Pedigree of family 1 and homozygosity mapping 21

Structure - function relationships of *PGM1*-mutations

Fig. S6 Details on PGM1 structure and mutations 24
Fig. S7 Real-time PCR for quantification of PGM1-mRNA in fibroblasts 25
Fig. S8 Western blot of PGM1 from PGM1 deficient fibroblasts 26

Fig. S9 Western blotting of fibroblast ICAM-1 27

Effects of galactose supplementation

Fig. S10 Galactose and uridine supplementation in patient fibroblasts 28
Fig. S11 Dietary effect of galactose on transferrin-glycosylation 29
Fig. S12 Effects of dietary galactose on total serum glycome 30

Fig. S13 Performance of Guthrie screening assay for PGM1-deficiency 31

Supplementary Tables

Table S1 Biochemical and clinical features in PGM1 deficiency 32
Table S2 Primers used for PGM1 sequencing 33
Table S3 Glycogen content in patient fibroblasts 35
Table S4 Range of GALT-, PGM-, and G6PDH-activities of 8 patients with PGM1-deficiency and healthy newborns 36

References 37

Responsibility for manuscript content and data evaluation

All equally contributing first and senior authors jointly wrote the first draft and final manuscript, with substantial contributions from the coauthors, and decided to submit the manuscript for publication. They assume responsibility for the overall content and integrity of the manuscript. All authors vouch for the accuracy and completeness of the reported data.

SUPPLEMENTARY METHODS

Homozygosity mapping: mapping the disease locus by linkage analysis

For homozygosity mapping, 400 ng DNA from each of the two affected sibs of the inbred pedigree shown in Fig. S5A was used. Illumina 1M Duo beadchips were processed according to the manufacturer's instructions. The data presentation by Illumina Genomestudio software enabled us to depict the borders (RS-IDs of markers) of homozygous regions by visual inspection. In addition we calculated lod scores over the chromosomes using Merlin-1.1.2 software.[1] The result for chromosome 1 is shown in Fig. S5B and the other chromosomes follow in Fig. S5C.

Since in the pedigree the effective number of meioses is 6, a maximum lod score value below $\log_{10}(2^6) = 1.8062$ could be expected (limit for disease freq → 0 and SNP allele frequencies → 0). After providing Merlin with quality filtered Illumina-data from the two affected sibs (~380000 SNPs), the pedigree structure, real SNP-allele frequencies, and a model file for recessive disease with disease frequency set to 0.0001, lod scores were calculated. A maximum lod score of 1.8057 was obtained. Lod score results below -12 were set to -12. Data were further processed using visual basic code to extract all those homozygous regions with a size of more than 1 Mb. To this end, the lod scores were dichotomized (1 vs. 0) using a cutoff 1 lod unit below the maximal limit of 1.8062, i.e. 0.8. Then the homozygous regions were determined as regions of at least 1 Mb containing no "0" and finally the first heterozygous marker adjacent to each end of a homozygosity region was selected as the limit of the homozygous region. Occurrence of two singular heterozygous SNPs, one in each of two large homozygous regions, (15 Mb on chr. 1, and 40.6 Mb on chr. 10) were not considered as interruption of the homozygous regions. This conclusion is based on the normal human mutation frequency (1-$2.5/10^8$ basepairs per meiosis[2,3]) and the pedigree structure (distance of 4 meioses between the parents of the affected sib pair); with these parameters about 0.6-1.5 mutations/15 Mbases present in one of the parents are expected. One of these SNPs is visible in Fig. S5B about three megabases downstream of the PGM1 locus as a spike, down to a lod score < -8. By the homozygosity mapping, the candidate region could be reduced to 87.37 MB using actual Ensembl-release 69 data, scattered over the autosomal chromosomes in 12 regions.

Whole exome sequencing: identification of defective *PGM1*

For whole exome sequencing, genomic DNA was isolated from 8 ml of blood using PAXgene Blood DNA system (www.preAnalytiX.com). DNA quality was checked photometrically, and concentration was measured using the Qubit system (Qubit 2.0 fluorometer). DNA was processed following the Agilent SureSelect protocol. 3 µg DNA were sheared using a Covaris S2 (Covaris, USA) to obtain fragments around 200 bp. The Agilent protocol for selection of the exonic sequences was performed almost exactly as given, except that a BioRad Experion was used for QC steps during the process, including calculation of the final concentration of the library. A 10 nM sample-DNA dilution in Tris-HCl 10 mM, pH 8.5 with 0.1% Tween 20 buffer was further processed according to Illumina protocols, spiked with 1% PhiX-DNA as internal quality control. Cluster generation was performed on the flowcell using an Illumina cBot. Next generation sequencing was started on an Illumina HiScanSQ (paired end mode, 2 x 101 bases). Primary output (.bcl files) was transformed to -qseq.txt files using the Illumina BCL-converter. These files were mapped to the reference sequence comprising PhiX and the whole human genome (hg19), but excluding PAR regions on the Y-chromosome, using CLC Bio software. After SNP-calling, the respective data were exported and reimported into a Microsoft access database.

62973 variants from CLC were obtained. Using a table containing the limits of the candidate regions obtained by homozygosity mapping, the 1516 variants in these regions were selected and exported into a text file suitable for analysis by the Seattle SNP annotation software (http://gvs.gs.washington.edu/SeattleSeqAnnotation/). 1506 of the variants were single base substitutions comprising 164 missense, 2 nonsense, and 0 splice site mutations. 10 variants were indels (insertion/deletion mutations). Regarding the indels, one was false positive due to read-through into the primer region, three were known variants, one fitting 100% to alternate assembly and two with reported minor allele frequencies of 18 and 49 % respectively. The 1506 single nucleotide substitutions were further analyzed for minor allele frequency (MAF), and all showing MAF > 1.4% were removed (corresponding homozygosity freq. $0.014^2 \approx 1/5000$ i.e. definition of rare diseases). To determine the minor allele frequencies, HapMap-frequencies and Exome Sequence Project-data (automatically extracted via http://snp.gs.washington.edu/SeattleSeqAnnotation134/) as well as MAF-data obtained via Biomart from the Ensembl database were used. 168 variant positions remained after application of the MAF > 1.4% cutoff. Next, we filtered off variants that were designed as intron / intergenic / outside coding / coding-synonymous etc., and those where Chimp allele was same as patients sample allele were also excluded. By this procedure the dataset was reduced to 10 variants in 10 genes (HGNC-symbols): *PGM1*, *LRRC40*, *PAPOLG*, *RIOK1*, *GCNT6*, *PDE6C*, *HPSE2*, *DCLRE1A*, *PDZD8*, *PRDX3*.

The functional description suggested a relation to glycosylation for *PGM1* and *GCNT6* only. Inheritance of both variants was checked in the family. The *PGM1* variant was homozygous in the two affected patients only (parents were heterozygotes, Fig. S5A), while the *GCNT6*-variant was also detected in homozygous form in an unaffected sib. We confirmed *PGM1* as the

defective gene in additional individuals with similar IEF-patterns . All identified mutations were not reported in dbSNP or Exome Sequencing Project of 6500 exomes. Functional relevance was demonstrated by a strong reduction in PGM1 enzymatic activity for all patients in respective material (fibroblasts, muscle cells, lymphocytes; see activity results in Table S1).

In an independent approach, genomic DNA of patient 6 was extracted from fibroblast pellets according to the manufacturer's protocol using a Qiagen Mini kit (Qiagen), and was checked for DNA degradation on agarose gels. The exome was captured and enriched using a SureSelect human exome enrichment kit (Agilent). After amplification, samples were sequenced on a Solid4 sequencer (Applied Biosystems) and color space reads were iteratively mapped to the hg19 reference genome with the Solid Bioscope software version 1.3, as described previously.[4,5] After filtering against known SNPs and prioritization using a broader list of genes that included known CDG genes and additional other genes involved in sugar and nucleotide sugar metabolism[4], *PGM1* stood out as a primary candidate gene and was confirmed by enzyme activity measurement.

PCR and sequencing for mutation analysis

For sequencing of additional CDG patients, primers for genomic DNA and cDNA were designed with Primer3 software.[6] The samples, containing 1µl DNA (concentration range 10-80 ng/µl), 2 µl PCR Buffer 10x (Qiagen), 2 mM dNTPs (GE Healthcare, Buckinghamshire, UK), 9 µl A. dest., 0.1 µl Taq DNA Polymerase (Qiagen), 1 µl primer forward and 1 µl primer reverse (20 pmol/µl), were cycled 35 times using the primers and conditions listed in Table S2.1 and S2.2 (this Appendix). Purification of the amplified DNA was done according to the manufacturer´s protocol of PCR Product Pre-Sequencing Kit (USB Corporation, Ohio, USA).

Sanger sequencing was performed using Big Dye Terminator Kit 3.1 (Applied Biosystems, Darmstadt, Germany) and MicroAmp Optical 96-Well Reaction Plate (Applied Biosystems) on an ABI 3730 XL capillary sequencer after purification with Sephadex on MultiScreen Filter Plates (Millipore Corporation, Billerica, USA).

Patient cells and tissues

Leukocytes were prepared from blood obtained by venipuncture for standard clinical laboratory measurements. For phosphoglucomutase 1 activity, **leukocyte** pellets were isolated from heparin blood by dextran precipitation according to routine laboratory protocols. Pellets were washed with PBS and frozen at -20 °C.

Fibroblasts were obtained by standard procedures from skin biopsies. In brief, a 2 - 4 mm skin punch are obtained under local anesthesia (EMLA-plaster, AstraZeneca) and added to a 15 ml centrifuge tube with 10 ml cell culture medium (MEM containing 1 g glucose/L, 1% of L-glutamine/streptomycin/penicillin mixture, and 10 % FBS; PAA laboratories). Under the sterile conditions, medium is removed and the specimen flushed with a small volume of fresh medium

into a 10 cm petri dish. The specimen is cut into 4-6 small pieces, that are placed into a 25 cm^2 cell culture flask with the subcutaneous fat region touching to the plastic surface. The flask is turned into a vertical position, filled with 5 ml culture medium and left in the vertical position for about 2 h in the incubator (37°C, 5% CO_2) to allow the skin pieces to get firm contact to the flask surface. Afterwards the flask is gently turned into horizontal position. Fibroblasts are allowed to grow out from tissue for 3-4 weeks, changing the medium once per week. The cells grown out from the tissue pieces are trypsinized, distributed within the same flask and allowed to further grow to confluence. From that point cells are split 1:3 about every 4 days. Cells are cryopreserved in 10 % DMSO / culture medium and placed at liquid nitrogen for long term storage.

To prepare cell pellets for later use in measurement of phosphoglucomutase 1 activity or nucleotide sugar analysis, cells were grown in culture to 80-90% confluence, were then trypsinized, pelleted, washed with PBS and pelleted again at 500 x g, 5 min. After removal of supernatant, pellets were stored at -20°C or in liquid nitrogen.

Further processing of cells for specific methods is described in the respective paragraphs for each of those methods.

Muscle biopsies were taken from vastus lateralis in a diagnostic setting, before PGM1 deficiency was identified. For later processing and measurements of enzyme activities muscle specimens were washed once with PBS and frozen in liquid nitrogen.

Liver biopsies were obtained for clinical reasons by standard procedures and were taken before the diagnosis of PGM1 deficiency was made.

Real-time PCR for quantification of PGM1 mRNA

An equivalent of 25 ng total cellular RNA was mixed with 9 µl Qiagen-Quantitect 2xSybr-Green real time PCR kit in a total volume of 18 µl; each primer was added at 0.2 µM final concentration. Triplicate measurements were performed in an ABI3700 realtime cycler (Applied Biosystems/Invitrogen) programmed at15 min 95°C, 5 x (15 sec 95°C, 30 sec 60°C, 30 sec 72°C), 40 x (15 sec 95°C, 1 min 60°C, 30 sec 72°C). Primers used for normalization were for *PPIA* from Biomol. *PGM1* primers spanning Exon8-Exon9 were 5'-AAAGATGGACTGTGGGCTGTCCT and 5'- CCTCAGCTTCCACCTCCTCGTAA.

Western blotting for PGM1

For Western blots, fibroblast pellets were washed in PBS (phosphate buffered saline; PAA, Cölbe, Germany), centrifuged (5 min, 500 x g, room temperature) and resuspended in HEPES-sucrose-buffer (0.2 M sucrose, 0.02 M HEPES, pH 7.3) supplemented with protease inhibitors (Complete, Roche; 10 µg/ml pepstatin A; 10 µg/ml PMSF). Fibroblasts were disrupted with a Dounce homogenizer. Homogenate was centrifuged at 3000 rpm at 4 °C for 15 min to make the

cytosolic fraction, whose protein concentration was determined using Bradford assay. Sample was adjusted to 0.5 µg/µl with loading buffer, heated at 95°C for 5 min and 2 µg of each sample was used for SDS-PAGE (10 % solving gel). PageRuler protein ladder (Fermentas, St. Leon-Rot, Germany; SM0671) served as a molecular weight standard.

After separation, proteins were transferred to Immobilon-P filters, (Millipore GmbH, Schwalbach/Ts., Germany) via Trans-Blot SD Semi-Dry Transfer Cell (Bio-Rad Laboratories GmbH, Munich, Germany) for 1 h at 10 V.

Membranes were blocked overnight with 5 % milk powder (Carl Roth GmbH, Karlsruhe, Germany) in PBST buffer (PBS supplemented with 0.1 % Tween; Merck Schuchardt OHG, Hohenbrunn, Germany) at 4°C, and incubated for 3 hr with 1:2000 diluted monoclonal anti-PGM1 antibody (ab55616; abcam, Cambridge, UK) in PBST (+ 5 % milk powder). After washing 3 x 10 min with 20 ml PBST each, the membrane was incubated with a 1:2000 dilution HRP conjugated polyclonal rabbit anti-mouse antibody (Dako, Glostrup, Denmark; P0260) in PBST (+ 5 % milk powder) for 45 min at room temperature. 4 x 10 min washes at room temperature was followed by the detection of PGM1 using Immobilon Western Chemiluminescent HRP Substrate (Millipore Corporation, Billerica, USA) on a high performance chemiluminescence film (Amersham, GE Healthcare, Munich, Germany). Exposure time was approximately 10 min.

Phosphoglucomutase 1 enzyme activity

Cell extracts were prepared from **fibroblasts** or **leukocytes** by thawing a frozen cell pellet in 200 µl of 20 mM Hepes, pH 7.4, containing 1 mM dithiothreitol, 5 µg/ml leupeptin and 5 µg/ml antipain. The cell homogenates were centrifuged for 2 min at 10,000 x g and supernatants used for enzymatic and protein assays. Protein was assayed with the Lowry method[7] using bovine serum albumin as a standard. Phosphoglucomutase was assayed spectrophotometrically at 30 °C, in assay mixtures comprising 100 mM Tris, pH 7.4, 7.5 mM $MgCl_2$, 25 mM KCl, 1 mM dithiothreitol, 0.25 mM NADP and 0.35 U of yeast glucose-6-phosphate dehydrogenase. The phosphoglucomutase assay also included 1 mM glucose-1-phosphate and 10 µM glucose-1,6-bisphosphate. Blanks were run in the absence of the substrate. The assay was initiated by the addition of an appropriate volume (2-5 µl) of an extract containing 5-15 mg protein/ml.

Similarly PGM1-activity from **muscle tissue** was measured with following modifications:
Muscle specimens previously stored in liquid nitrogen were thawed. Muscle homogenate (1:10 w/v) was prepared in a buffer composed of 0.025 mM triethanolamine-hydrochloride, 1.25 mM EDTA, 1 mM ß-mercaptoethanol, pH 7.5, with mortar and pestle. After centrifugation (5 min at 8,000 x g), the supernatant was 1:4 diluted in the same buffer.

Phosphoglucomutase was assayed spectrophotometrically at 340 nm and at 25°C. Twenty-five µl of muscle homogenate were mixed with 1975 µl of a mixture containing (final concentrations) EDTA (4.2 mM), $MgCl_2$ (10 mM), NADP (0.57 mM), glucose-1,6-diphosphate (15 µM),

glucose-6-phosphate dehydrogenase (875 U/l), glucose-1-phosphate (3.5 mM) and triethanolamine-hydrochloride buffer pH 7.5 (85 mM). Blanks were run in the absence of substrate. The assay was initiated with glucose-1-phosphate.

Assays of transferrin glycosylation

The standard assay for measuring transferrin glycosylation is **isoelectric focusing**, which can show a deficiency in protein N-glycosylation, due to a reduced number of the terminal sialic acids. Interpretation of results is supported by **SDS-PAGE** which shows changes in the protein mass of transferrin, if whole glycans are missing, i.e. the method indicates unoccupied glycosylation sites. **QTOF mass spectrometry of intact transferrin** can reveal more detailed changes in the glycan structure**.**

Isoelectric focusing of transferrin

Isoelectric focusing of serum transferrin (IEF) is used as a measure for the general efficiency of the protein N-glycosylation process. Transferrin is a glycoprotein produced in the liver containing two N-linked oligosaccharides with two negatively charged terminal sialic acids each (tetrasialotransferrin). Due to its electric charge, transferrin migrates through an agarose gel (agarose for IEF, GE Healthcare Bio Sciences AB, Uppsala, Sweden) prepared with ampholines with a pH range of 5.0-7.0 (GE Healthcare Bio Sciences AB) and coated on Gel Fix plastic sheets (gel size 6.2 x 5 cm^2, Serva Electrophoresis GmbH, Heidelberg, Germany). To produce the gel, 2.2 ml of 1 % agarose with 110 µl ampholine, solved by heating is casted on the plastic support. Transferrin has two iron binding sites, which should be saturated with iron, so that different states of iron load cannot influence its migration behavior. Therefore, 10 µl serum are incubated with 66.6 µl 0.9% NaCl, 2.3 µl 10 mM Fe(III)citrate and 2.3 µl 0.1 M $NaHCO_3$. The iron-saturated samples are applied to the IEF-gel automatically via the PhastSystem sample applicator (about 1 µl/sample) and separated by isoelectric focusing with the Pharmacia Phast system (Pharmacia Fine Chemicals, Uppsala, Sweden), The program for electrophoresis is 300 V for 40 Vh, 100 V for 10 Vh and 200 V for 65 Vh, cooled to 10 °C. For evaluation of data, healthy controls, CDG-I- and CDG-II samples may be loaded for comparison. The healthy controls have tetrasialotransferrin as the major band. The mechanism and effects of mutations leading to CDG-I and -II are explained in the main paper, Fig. 1.

For visualizing the bands the gel is carefully over layed with 80 µl of transferrin antibody (Polyclonal Rabbit Anti-Human Transferrin, A0061 Dako A/S, Gostrup, Denmark; undiluted, 15-30 min incubation) to allow building of transferrin-antibody complex precipitates within the gel. Afterwards other proteins are washed out by at least 1 h shaking or overnight incubation in 0.9 % sodium chloride solution in water. After a further wash for 10-30 minutes in distilled water, the gel is dried by application of blotting papers and weight for 0.5-1 h. Further drying is accomplished by application of a hair dryer for up to 1 min. For staining, the gel is incubated for

10 - 30 minutes in a solution of 1.5 g Coomassie R 250 in 300 ml destain (350 ml ethanol, 100 ml acetic acid, 650 ml distilled water). To remove excessive stain, the gel is destained with destain-solution 3 times for 10 min or more often until background color is removed and the transferrin signals are clearly visible.

Immunoprecipitation and SDS-PAGE of transferrin

5 µl serum was immunoprecipitated with 1 ml MNT buffer (20 mM 2-[N-morpholino]ethane sulfonic acid, 100 mM NaCl, 30 mM Tris-HCl, pH 7.5) containing 1 mg/ml albumin and 1 mM Fe(III)citrat, 3 µl rabbit anti-human transferrin antibody (DAKO, 1:1 with glycerin; A0061; DAKOPATTS, Copenhagen, Denmark) with 70 µl Protein-A-Sepharose 10 % (Sigma-Aldrich Chemie GmbH, Steinheim, Germany) and protease inhibitors (10 µg/ml of chymostatin, leupeptin, antipain and pepstatin A each). Samples rotated for 4 hours at 4 °C and were then washed once with MNT buffer and afterwards twice at room temperature with 1 ml 0.05% TX-100, 0.1 % SDS, 0.3 M NaCl, 0.02 % NaN_3, 10 mM Tris, pH 8.6.

40 µl sample buffer (45 g 9 % SDS, 75 g 15 % glycerol, 15 ml 1M 30 mM Tris-HCl pH 7.8, 0.25 g 0.05 % bromphenolblue, 500 ml H_2O) was added to the immunoprecipitated samples. After boiling, this was run on a 7.5 % polyacrylamide gel (Rotiphorese Gel30, Carl Roth, Karlsruhe, Germany) at 150V in an electrophoresis chamber (Se250 Mighty Small II; Hoefer Scientific Instruments, San Francisco, USA). Afterwards, the gel was stained in 0.5 g Coomassie Blue R 250 (Sigma-Aldrich, Steinheim, Germany) dissolved in 800 ml methanol, 800 ml H_20 and 200 ml 100 % acetic acid.

QTOF mass spectrometry of intact transferrin

For high-resolution mass spectrometry of transferrin (Fig. 3 main text), a 5 µl serum sample was incubated with anti-transferrin beads as described.[8] The eluate was analyzed on a microfluidic 6540 LC-chip-QTOF instrument (Agilent Technologies) using a C8 protein chip. Data analysis was performed using Agilent Mass Hunter Qualitative Analysis Software B.04.00. The Agilent BioConfirm Software was used to deconvolute the charge distribution of raw data to reconstructed mass data. For confirmation of the structural annotations, samples were processed for analysis of tryptic transferrin peptides by MALDI-TOF as described[9] (results not shown).

Western blotting for ICAM-1

Western blotting of ICAM-I (Fig. S9) was performed as described.[10] In brief, approximately 20 µg of protein lysate from each sample were separated on SDS-PAGE and then transferred to nitrocellulose membranes. After blocking, the membranes were incubated with Goat Anti-mouse ICAM-1 antibody (AF796, R&D Systems, Minneapolis, MN) at 1:500 dilution. Following intensive washing, the membranes were developed with secondary antibodies and visualized using ECL system with higher sensitivity (Immun-Star WesternC Kit, Bio-Rad, Hercules, CA).

Assay for cellular glycosylation efficiency using modified GFP

Glycosylation efficiency was measured using Glyc-ER-GFP constructs as described.[11] In brief, cells were seeded in a 96 wells-plate at 40% confluence. 24h later, they were incubated in medium without or with addition of supplements (e.g. 0-1 mM galactose +/- 100µM uridine) for 2 days with medium replacement every day. Cells were then transfected by the Glyc-ER-GFP and maintained in the same culture media for two more days. Cells were fixed using 4% paraformaldehyde/4% sucrose and stained by Hoechst 33342 (Thermo scientific). Plates were analyzed using a high-content microscope, IN Cell 1000 (GE Healthcare), and data were analyzed with the CytoSeer software (Vala Sciences) using a protein mask.

Nucleotide sugar assay

Nucleotide sugars were extracted from fibroblast pellets that had been stored at -20 °C. 900 µl ice cold 85 % ethanol and 120 µl PBS were added, and after sonication, cellular debris was removed by centrifugation at 13000 rpm, 10 min. The supernatant was evaporated in a SpeedVac concentrator and resuspended in 1 ml water. Insoluble material was removed by centrifugation and supernatant mixed with 50 µl 0.2 M NH_4HCO_3. The sample was further purified by an Envi-Carb carbon column according to the method of Rabina[12] and UDP-galactose and UDP-glucose were measured by reverse phase HPLC on an Inertsil ODS-4 column according to Nakajima at 254 nm.[13]

Phosphorylated sugar assay

Galactose-1-phosphate was exactly measured as described by Shin YS.[14].

For measurement of **glucose-1-phosphate**, fibroblast cell extract was prepared according to Donthi et al.[15]. Glucose-1-phosphate was measured by employing a coupled enzyme assay using phosphoglucomutase 1 and glucose-6-phosphate dehydrogenase with a fluorescent readout. Briefly, 20 µl cell extract for each sample was dispensed in the wells of a black assay plate. Depending on the number of samples, two sets of reaction mix were prepared containing 50 mM HEPES, 1 mM magnesium chloride, 100 mM NADP, 10 mM resazurin, 0.25 units diaphorase, 10 mM glucose-1,6-bis-phosphate in a total volume of 80 µl per sample. Phosphoglucomutase 1 and glucose-6-phosphate dehydrogenase (0.25 units each/sample) were added to one set (F2) and only glucose-6-phosphate dehydrogenase (0.25 units each/sample) was added to the other set

(F1). Another mix (Fb) containing glucose-6-phosphate dehydrogenase, but devoid of NADP was prepared to determine the background due to endogenous NADP in each sample. 80 µl of the reaction mix was added to the respective wells containing 20 µl of the extract and incubated in dark at room temperature. Fluorescence was recorded at excitation wavelength 530 nm and emission at 590 nm using Flexstation III (Molecular Devices, Sunnyvale, CA, USA). Background fluorescence (Fb) was subtracted from all the samples (F2 and F1). Difference between the fluorescence values (F2-F1) was used to calculate pmols of glucose-1-phosphate from the standard curve generated by known amounts. The results of reaction set F1 were used to calculate **glucose-6-phosphate** levels.

Biochemical quantification of glycogen

Glycogen was extracted from fibroblasts and digested with amyloglucosidase according to the methods of Passonneau.[16] Total amount of glucose was analyzed by GC/MS. Glucose derived from glycogen was calculated as difference compared to non-treated samples. Results are expressed as glycosyl unit per mg protein according to the method by H.M. Sickmann.[17]

Evaluation of glycogen by electron microscopy

For electron microscopy, skin fibroblasts of patients and controls were cultured to a confluence of 50 to 70% in M199 medium (Life Technologies) supplemented with 10% fetal calf serum and 1% penicillin/streptomycin in a humidified atmosphere containing 5% CO_2 at 37°C. Cells were switched to a medium consisting of DMEM supplemented with 4mM L-glutamine (Invitrogen), 10% dialyzed FCS (Gibco), 1mM uridine (Calbiochem), and either 5.5 mM D-glucose (Sigma), or 5.5 mM D-Galactose (Merck). After 50 h of incubation, cells were centrifuged for 10 min at 1000rpm and fixed by gentle addition of 2% glutaraldehyde buffered with 0.1 M sodium cacodylate pH7.4 after removing the medium. After at least 4h fixation, the pellets were very carefully taken off and post-fixed in 1% osmium tetroxide in Palade buffer pH 7.4 with 1% potassium hexacyanoferrate(III)-trihydrate, and after dehydration in ethanol and propylene oxide, embedded in Epon for electron microscopy. Semithin 1µm thick transverse sections were stained with 1% Toluidine Blue. Ultrathin sections were stained with uranyl acetate and lead citrate and examined on a JEOL 1200 EX\II. Most control cells showed fine diffusely dispersed glycogen. Cells with small darkly staining aggregates of glycogen were counted as positive. For each cell line, more than 110 cells were counted and the percentage of positive cells is presented in Table S3.

Determination of galactose kinetics in whole blood

Enzymatic determination of galactose levels in whole blood was performed using exogenous galactose dehydrogenase (galactose + NAD^+ → galactono-1,4-lactone + NADH + H^+). Galactose levels were determined in a healthy control after oral consumption of 0.3 g galactose (falcento AG, Kreuzlingen, Switzerland) per kilogram body weight dissolved in 250 ml water.

Measurements of galactose levels were made at intervals of 10 minutes during the first hour and at intervals of 30 minutes for additional three hours.

3000 µl of galactose buffer reagent (Instruchemie, Delfzijl, Netherlands), 100 µl of galactose NAD reagent (Instruchemie) and 200 µl of a diluted calibrator (Instruchemie) were mixed and the absorbance against distilled water was read at a temperature of 25 °C and a wavelength of 340 nm (optical density 1).

500 µl of each whole blood sample were added to 1000 µl perchloric acid (0.33 mol/l) for deproteinization and then centrifuged. 200 µl of the supernatant were added to 3000 µl galactose buffer reagent, 100 µl galactose NAD reagent and absorbance was read (optical density 1). After supplementation of 20 µl galactose start reagent and incubation at 25 °C for 15 min, the optical density 2 was measured in both, the calibrator and blood samples.

For manual calculation of the galactose concentration the following formula was used:

$$galactose\ (mmol/l) = \frac{\Delta O.D.\ control\ or\ sample}{\Delta O.D.\ calibrator} \times concentration\ of\ calibrator$$

SUPPLEMENTARY RESULTS

Clinical phenotype

Bifid uvula, a clinical manifestation atypical for CDG, was present in 16 patients, in two cases with cleft palate but without cleft lips.

Liver biopsy was performed in five patients showing steatosis, cholestasis, slight fibrosis and/or bile duct atrophy. An increased amount of glycogen was observed in only two of these patients by PAS staining. In one of these biopsies, electron microscopy revealed glycogen particles in hepatocytes, but much less than in other glycogen storage disorders (Supplement Fig. S3).

Heart: Three girls with severe DCM (2, 5.2, 6, numbers referring to Table S1) were temporarily listed for cardiac transplantation, but, surprisingly, cardiomyopathy in the first two improved with time. In patient 5.2 and males 3, 7, 14, cardiac arrest occurred, in 5.2 in the context of anesthesia (resuscitated), and in 3 at age 13 induced by exercise (running for his school bus). After resuscitation, he developed epilepsy, a severe ventilation disorder and had episodes of thrombosis. Patients 7 and 14 died at age 8 and 10, respectively, from a cerebrovascular accident and respiratory failure. Both suffered from end-stage DCM.

Electrocardiograms, where available, were checked for arrhythmias associated with DCM, but none were seen. In patient 2, infantile dilated cardiomyopathy (DCM) was diagnosed at 5 months; the lowest measured fractional shortening (FS) of 5% in this patient improved spontaneously to 13% and during complex carbohydrate supplementation to 24%. In patient 5.2,

at 16 months, after anesthesia for cleft palate surgery, cardiac arrest occurred. Shortly thereafter, DCM was diagnosed and at age 7 heart transplantation was recommended. However, her heart recovered significantly, with an adult FS at different timepoints of 24% - 33%. Her brother, patient 5.1, had a slightly enlarged left ventricle with normal function (FS 31%).

Growth: In several patients with **growth retardation**, where measured, IGF-1/IGFBP3 concentrations around the lower range of normal were observed, with normal or high excretion of growth hormone after provocation with arginine or insulin.

Other hormones: Low cortisol and ACTH concentrations were recorded in 2 patients. Activities of coagulation factors ATIII, factor XI, protein C, and protein S were reduced in half of the patients. In addition TSH, which shares one subunit with LH and FSH (see main text, reduced in two girls and associated with hypogonadotropic hypogonadism) was also observed to be low in several cases. All these mentioned hormones and coagulation factors are glycoproteins and have been reported to be affected in patients with CDGs.

Pseudocholinesterase (PCHE), a serum glycoprotein produced by liver, for which deficiencies may be associated with prolonged recovery after anesthesia, was measured in several patients and often found to be below the 2.5th percentile. The level was proportional to general glycosylation efficiency as estimated from transferrin glycosylation (to be published elsewhere).

Sugar metabolite and glycogen quantification

Determination of **galactose-1-phosphate** (Gal-1-P) levels revealed in the mean 3-fold elevated levels in PGM1-deficient fibroblasts vs. controls (14.4-24.1 nmol/mg protein, mean 18.77, n=6, in PGM1-deficient cells; 3.8-12.1, mean 6.96, n=7, in controls) but normal levels in erythrocytes. The normal Gal-1-P in erythrocytes is likely to be explained by the high PGM2 activity in erythrocytes. In agreement with this interpretation, glycosylation of erythrocyte band 3 glycoprotein was normal (data not shown).

Glucose-1-P content was about 10-fold higher in patient fibroblasts than in controls (mean 1.9 ± 0.5 nmol/mg protein, n=9, vs. 0.22 ± 0.12 nmol/mg protein, n=6), whereas glucose-6-P (n=9 vs. n=6) was normal in patient fibroblasts.

An increased **ratio of UDP-Glc:UDP-Gal** in patient fibroblasts vs. controls ($3{,}6 \pm 0.58$, n = 5, vs. $2{,}4 \pm 0.25$, n = 2) suggests that UDP-Gal might be limiting for complex N-glycan synthesis. The data are consistent with a glycogenolytic state of the cells, where Glc-1-P derived from glycogen is increased (due to the PGM1 defect it is not converted to Gluc-6-P). Via the GALT reaction, a portion of the Glc-1-P will react with residual UDP-Gal to increase UDP-Glc and Gal-1-P, leading to the observed metabolite changes in patients vs. control. The differences were mainly due to UDP-Gal with a level of 1150 ± 240 pmol/mg protein, n = 2, controls, vs. 710 ± 250 pmol/mg protein, n = 5, patient cells. UDP-Glc was not significantly different, 2720 ± 280 pmol/mg protein, n = 2, controls, vs. 2580 ± 1050 pmol/mg protein, n = 5, patient cells.

Adding galactose and uridine to PGM1-deficient cells normalized the ratio (n=4) and essentially improved glycosylation (Fig. S10), but left the ratio in control fibroblasts normal (n=3).

Glycogen levels in patient fibroblasts (137 ± 62 nmol/mg protein, n=5) were comparable to controls (118 nmol/mg protein, n=2). In addition, analysis of glycogen aggregates was studied by electron microscopy in fibroblasts. Culturing of cells in the presence of either 5.5 mM glucose or 5.5 mM galactose showed no accumulation of glycogen particles in PGM1-deficient fibroblasts (Table S3).

SUPPLEMENTARY DISCUSSION

Lack of effect of PGM1 deficiency on erythrocytes and the brain

Nearly all CDGs show multisystem manifestations, including effects on brain development. In contrast, PGM1-deficient patients have normal neurological function, which is likely a consequence of the presence of alternate enzymes providing PGM function in the brain. Phosphoglucomutases are a family of isoenzymes. PGM1 is expressed ubiquitously and is responsible for 80-95% of the total phosphoglucomutase activity in most tissues and even more in liver, cardiac muscle and white blood cells.[18] PGM2 is responsible for 50% of the total phosphoglucomutase activity in erythrocytes.[18] In brain, PGM2[19,20] and phosphomannomutase 1[21] account for the PGM activity, which is consistent with the absence of a neurological phenotype in PGM1-deficient patients.

Effect of reduced glycosylation on gonadotropin function: LH and FSH

The gonadotropins LH, FSH and their respective receptors are glycoproteins. LH and FSH are both heterodimers, that have in common a chain "C" with 2 N-glycosylation sites, while the β chains specific for the hormones have 1 (LH-β) and 2 (FSH-β) N-glycosylation sites (e.g. reviewed by Huhtaniemi[22]). There is no specific selection system in the glycosylation machinery that would lead, in patients with PGM1-deficiency, to preferential glycosylation of some specific proteins during the glycosylation process, but excluding LH, FSH etc (see Fig. 1 of main manuscript describing the general process of glycosylation; in addition Supplementary Fig. S12 on the effect of galactose supplementation, demonstrated that total serum glycoproteins are affected by underglycosylation and that this is reversed by galactose). Thus our data and all evidence from the previous literature suggest that underglycosylation of LH, FSH and their receptors occurs in PGM1-deficiency. The essential question of whether this has functional consequences has also been addressed in literature, and it has been reported that the half-life of underglycosylated LH and FSH is reduced[22]. The essential mechanism impeding LH function,

however, is that underglycosylated LH is still able to interact with the LH-receptor, but instead of regular signaling further signaling is blocked.[23]

For FSH, Galway AB et al. demonstrated that FSH molecules that have truncated glycans that lack only the sialic acids, or those from patients with an early block of CDG-I-type (MGAT1-deficiency) leading to only partially synthesized glycans, are still able to bind the receptor and elicit a response in vitro.[24] However, they demonstrated that injection into rats resulted in readily measured estrogen production with wild type FSH, but no response with the variant FSH forms. In a bioactivity assay, injection of wild type FSH resulted in a strong signal for 6-12 hours, while injected variant forms showed no signal at 3, 6, 12, and 24 hours. Thus, the activity half-life of underglycosylated FSH is significantly reduced.

Since we were able to demonstrate an improvement in general glycosylation efficiency with galactose supplementation, our data in combination with evidence from literature suggest, that the observed onset of puberty soon after galactose supplementation in both hypogonadotropic hypogonadic females is likely to be a direct consequence of improved glycosylation of LH and FSH, improving both the half-life and the in vivo function of these hormones.

Effect of reduced glycosylation on IGF1, IGFBP3, IGF-receptor and growth

Fifteen of 19 patients had short stature with height below the 5th percentile and showed reduced insulin-like growth factor 1 (IGF1) and its binding protein (IGFBP3).The physiologically relevant ternary complex is composed of IGF-1, IGFBP3 and the acid labile subunit (ALS). Miller et al. observed, by analyzing serum from 12 CDG-children (vs. 11 controls), significantly reduced serum levels of IGF-1, IGFBP3 and ALS.[25] While IGF-1 is a 70 amino acid peptide that is not glycosylated, most IGF-1 is bound in a functional ternary complex with IGFBP3 and ALS. The latter two carry 3 and 7 N-glycosylation sites respectively. Underglycosylation reduces the stability, the half-life and finally the concentration to about 50% of controls. The CDG-children showed significant growth retardation. While Niehues earlier demonstrated that mannose will correct glycosylation deficiency in CDG-Ib disease[26], Miller showed that mannose supplementation in CDG-Ib not only improves the glycosylation and normalizes the IGF-1, IGFBP3 and ALS levels, but also elicits a catch-up growth into the normal range. The mechanism leading to the growth effect, however, is not only the increased IGF1 level, but also essential improvement of the IGF1-receptor, a glycoprotein with 32 N-glycosylation consensus sites. As demonstrated by Carlberg et al. the IGF-1 receptor must be N-linked glycosylated in order to be translocated and expressed at the cell surface.[27]

Thus, supplementation of mannose in CDG-Ib significantly improves N-glycosylation, and in this way it restores IGF-1/IGF1-receptor function and normal growth.

In PGM1-deficiency, we have shown that IGF1 is reduced, as in CDG-Ib children. There is no reason to assume that ALS, IGFBP3 or IGF1-receptor should be exceptions regarding glycosylation if there is a general defect in glycosylation, as in PGM1-deficiency. Since we have demonstrated that galactose can improve significantly glycosylation, it is justified to assume that

the glycoslyation of the mentioned proteins involved in IGF1-function may be corrected by galactose supplementation and that, as in CDG-Ib, improved glycosylation will also improve growth. This conclusion is awaiting confirmation in a prospective study with compliant patients at an appropriate age.

Dilated cardiomyopathy: loss of functional interaction of PGM1 and ZASP

The involvement of heart due to dilated cardiomyopathy (DCM) was one of the most clinically important phenotypes associated with *PGM1* defects. Five of 19 patients suffered DCM and three of them experienced a cardiac arrest; one additional patient had a cardiac arrest due to vigorous exercise. The observation that loss of phosphoglucomutase 1 function can be associated with DCM has been made earlier by Arimura et al. Previously, Vatta et al. discovered that mutations in exon 4, 6 or 10 of the Z-disc protein ZASP were associated with dilated cardiomyopathy (DCM).[28] Arimura observed that most ZASP mutations related to DCM occured in exon 4 or 10.[29] They reported that ZASP has alternatively spliced isoforms and that exons 4 and 10 are preferentially expressed in the heart, while transcripts containing exon 6 are more specific for skeletal muscles. Since production of ZASP protein was not affected by some mutations in exons 4 and 6, they started a search for interaction with other proteins that might be disturbed by the mutations. They identified PGM1 binding to regions in ZASP encoded by both exons 4 and 10. They concluded that the lack of local presence of PGM1 in the Z-disc is involved in the pathogenesis of DCM.[29] Our study demonstrates that this may be the case, since defects in the PGM1 itself are also associated with DCM. Although there is a marked reduction of PGM1 activity in all patients, the clinical phenotype is variable. Severe DCM has considerably improved over time in two patients, suggesting that age, lifestyle, and nutrition may have a modulating impact. In cultured cardiomyocytes of rats, PGM1 is normally diffusely distributed in cytoplasm and not bound to ZASP.[29] Only after creation of defined stress conditions, by removing glucose or serum from the culture medium, is PGM1 bound to ZASP in the Z-disk. Anaerobic conditions in which ß-oxidation is not possible may require ZASP-PGM1 interaction, and the hypoglycemic periods observed in our patients may contribute as well. However, stabilizing glucose homeostasis by complex carbohydrates and restricting exercise to below the aerobic threshold should be beneficial.

If DCM is progressive, heart transplantation may be life-saving. Since the expression of normal PGM1 in the transplanted heart will restore locally the normal PGM1-ZASP-interaction, it can be assumed that the new heart will be protected from DCM in the PGM1-deficient patient.

SUPPLEMENTARY FIGURES

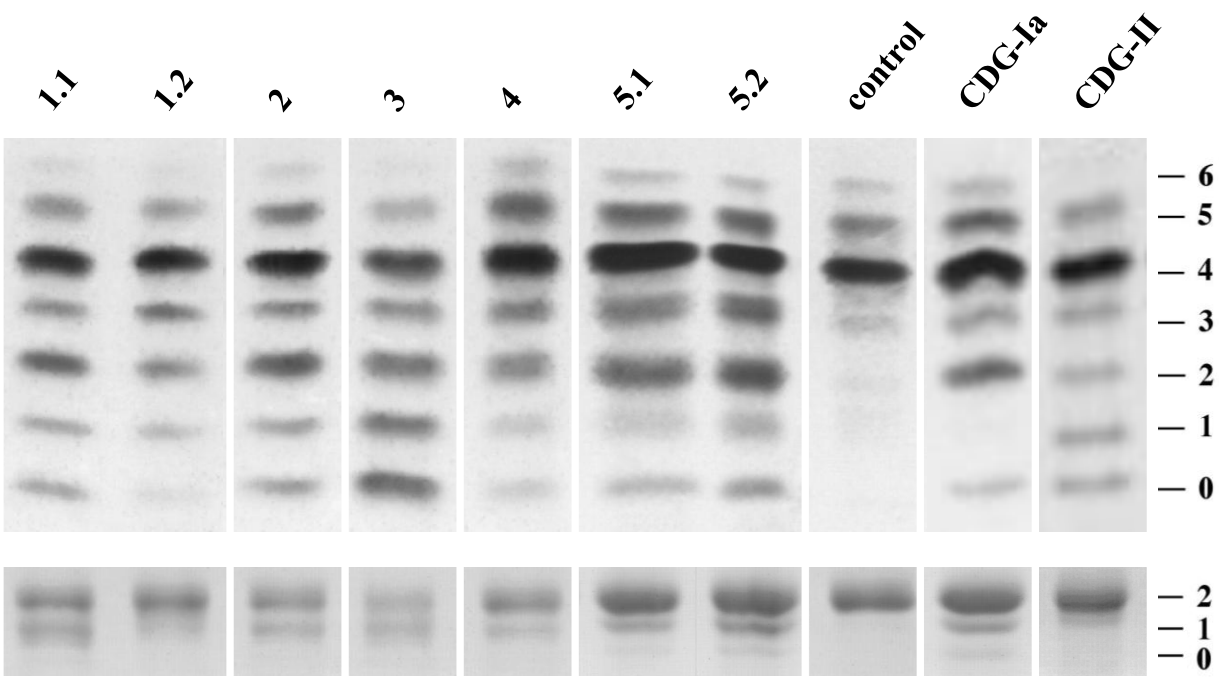

Figure S1. Isoelectric Focusing and SDS-PAGE of Transferrin.

In most patients, IEF showed a CDG-II like pattern with increased amounts of all hyposialylated transferrin isoforms and a decreased amount of the fully glycosylated tetrasialo-transferrin (top panel, number of sialic acids at right side, compare Fig. 1 in main text). SDS-PAGE (lower panel) provides additional information: Transferrin with both glycosylation sites occupied by a glycan was the major signal in most patients (position label "2" at right side: number of glycosylation sites occupied by a glycan). A molecular weight loss of 2 kDa corresponding to the complete lack of one oligosaccharide side chain suggested also a CDG-I-component (position label "1"). Also visible**:** loss of 4 kDa due to both glycosylation sites unoccupied in CDG-Ia positive control lane (position label "0"). Since transferrin with 1 sialic acid (position labeled 1 at top panel) is due to CDG-II defect, i.e. incomplete modification of already transferred glycan chain, patients have a mixed type of CDG-I and -II. Multiple smaller fuzzy bands in the lower panel represent truncations of the side chains. Individuals 1.1 and 1.2 as well as 5.1 and 5.2 are sibs indicating that variability of transferrin glycosylation may occur within sib pairs carrying the same mutations: 1.2 and 5.1 show a relatively less intense CDG-I-component in IEF (signals at 2 and 0) and SDS (signals at 1 and 0) than their respective sibs. Additional IEF patterns of patient 6 and 8 are shown in Fig. S4. Patient numbers are used as in Table S1.

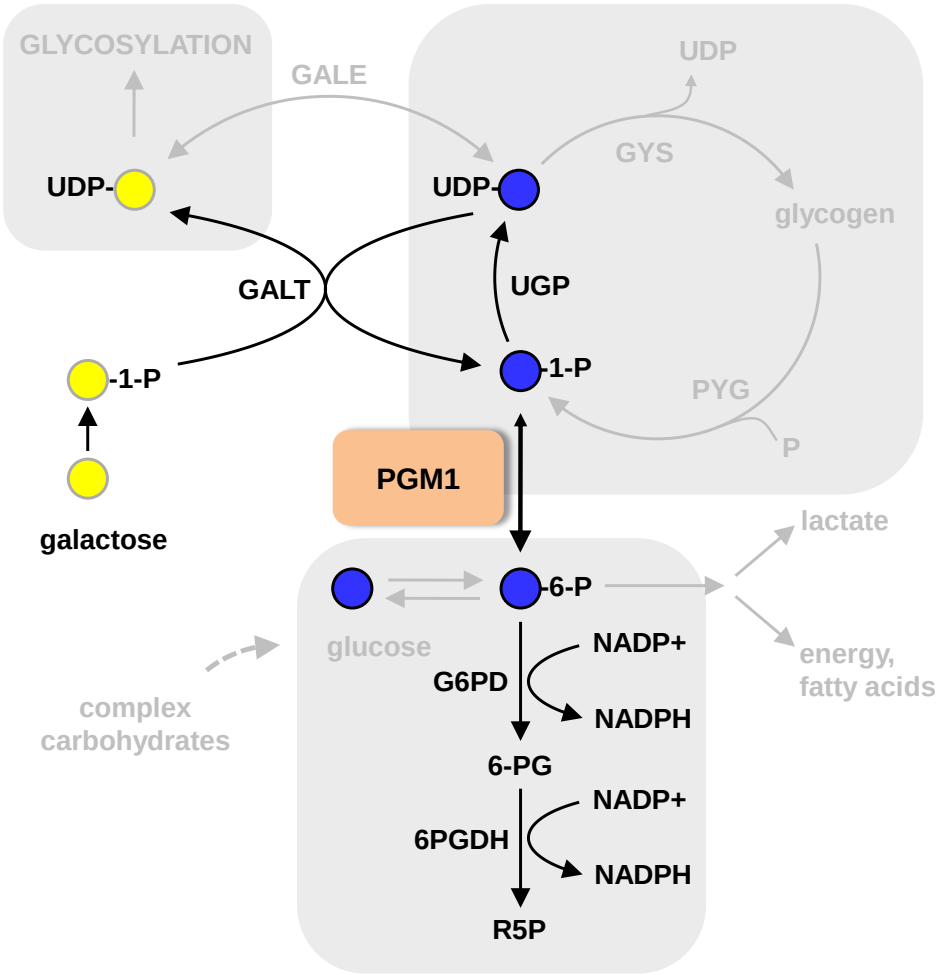

Figure S2. The Beutler Test and the Modified Beutler Test.

In this figure, the metabolic pathways for glucose and galactose that are of direct relevance to phosphoglucomutase 1 (PGM1) deficiency are shown as in Figure 2 in the main text, but parts not relevant for the test are dimmed. However, the further metabolic pathway down to ribulose-5-phosphate (R5P) that is also relevant for the Beutler test and the modified Beutler test is now also shown. In the Beutler test for galactosemia, the substrates galactose-1-phosphate and UDP-glucose are included in the test reagent and used to assay Guthrie heel prick test cards spotted with the patient's blood sample. In the presence of GALT, these substrates generate glucose-1-phosphate, which is then converted to glucose-6-phosphate by PGM1, then to 6-phosphogluconate by G6PD (glucose-6-phosphate dehydrogenase) and then to ribulose-5-phosphate by 6PGDH (6-phosphogluconate dehydrogenase). Each of these last two reactions is coupled to the conversion of NADP+ to NADPH. The fluorescence of NADPH is used as the basis for the Beutler test assay. Thus the Beutler test requires the presence of several functional enzymes including GALT, PGM1, G6PD, and 6PGDH (although in general the rate-limiting enzyme is GALT). In a modification of the Beutler test evaluated in this study, galactose-1-phosphate and UDP-glucose were replaced by glucose-1-phosphate as the assay substrate. A similar assay was also developed using glucose-6-phosphate as the assay substrate in order to bypass PGM1.

Keys: ● = glucose, ● = galactose, PGM1 = phosphoglucomutase 1, GALT = galactose-1-phosphate uridyltransferase, GALE = UDP-galactose epimerase, UGP = UDP-glucose pyrophosphorylase, GYS = glycogen synthase, PYG = glycogen phosphorylase, G6PD = glucose-6-phosphate dehydrogenase, 6-PG = 6-phosphogluconate, 6PGDH = 6-phosphogluconate dehydrogenase, R5P = ribulose-5-phosphate.

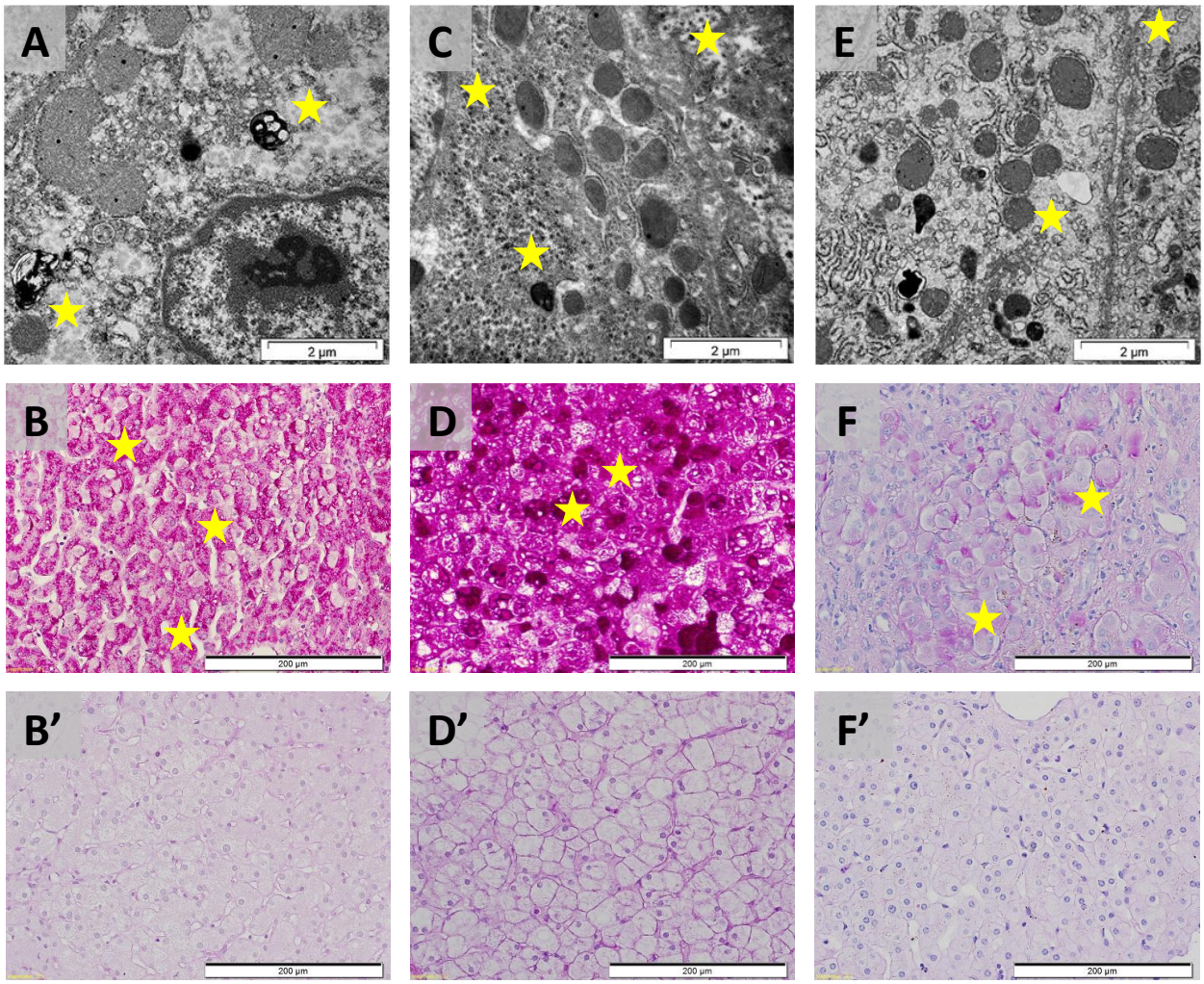

Figure S3. Glycogen in Hepatocytes by Electron Microscopy and Light Microscopy. Liver tissue sections for electron microscopy (EM) were obtained from samples fixed in 2.5% glutaraldehyde in 0.1 M cacodylate buffer, post-fixed in buffered 2% osmium tetroxide, and processed to Epon 812. Sections routinely stained for EM with uranyl acetate and lead citrate were analyzed with a Jeol Jem 1011 transmission microscope equipped with digital camera. Tissue samples for light microscope (LM) were fixed in 4% buffered formalin and processed to paraffin blocks. De-paraffinized 5 µm thick control sections were diastase treated and stained by periodic acid-Schiff reaction (PAS). (A,B) PGM1-deficient hepatocytes (patient 6) showing glycogen particles (pale material, asterix) in the cytoplasm in EM (A), and under LM in PAS stained sections (B) less abundant than in glycogen storage disease Ia (GSD-Ia) (C,D) but more abundant than in controls with for example liver cholestasis (E,F). Glycogen in GSD-Ia is increased and stained darker than in PGM1-deficiency, in addition dark dots of glycogen aggregates are visible (C). (B',D',F') Lack of glycogen particles on sections diastase treated and PAS stained, respectively liver of patient with PGM1-deficiency, GSD-Ia and cholestasis.

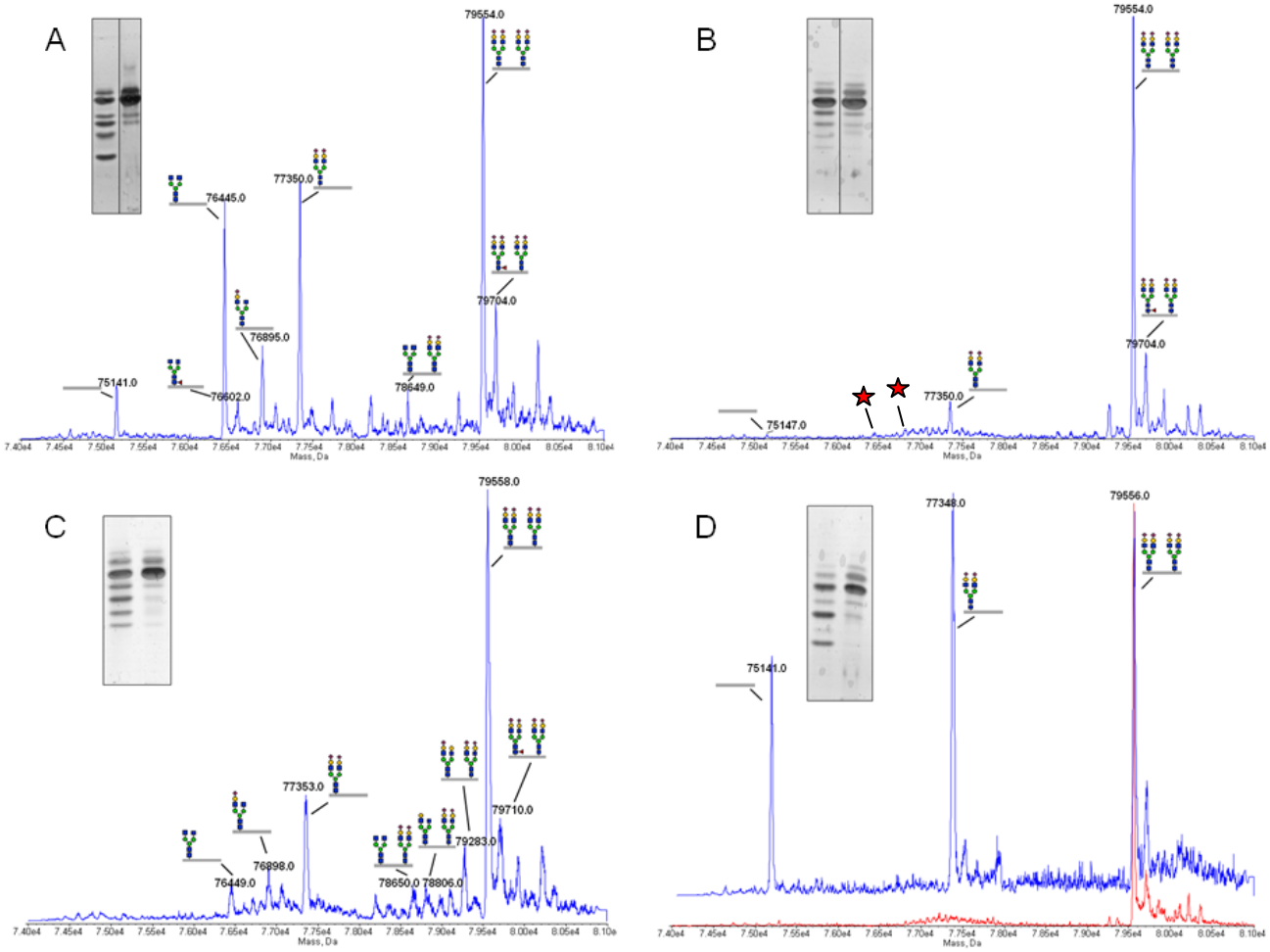

Figure S4. Variability of Transferrin Glycosylation, Details by Mass Spectrometry.

While the CDG-Ia aberrant pattern in panel D is demonstrated clearly by the two structures showing loss of one or both complete glycans, the PGM1-deficient patients show a variable mix of those two structures and other peaks where the glycans are lacking galactose and sialic acid, i.e. they show a mixed type CDG-I/II. The degree of glycosylation deficiency is also highly variable.

Panels A, B and C show spectra of the three PGM1 patients 6, 8, and 1.2 respectively. Panel D shows an overlay of a control (red) and CDG-Ia patient (blue). Corresponding transferrin isoelectric focusing gels are shown in the first lane. In the second lane a control sample is depicted as reference (panels A-C). In panel D, the first lane corresponds to the blue tracing, the second lane with the red spectrum. The symbol "★" indicates the presence of truncated transferrin glycans for patient 8. Gray bars indicate the transferrin protein backbone.

A

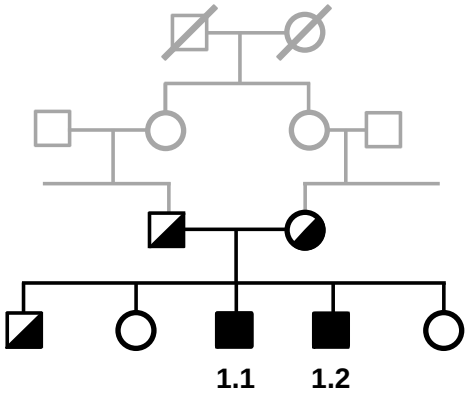

B

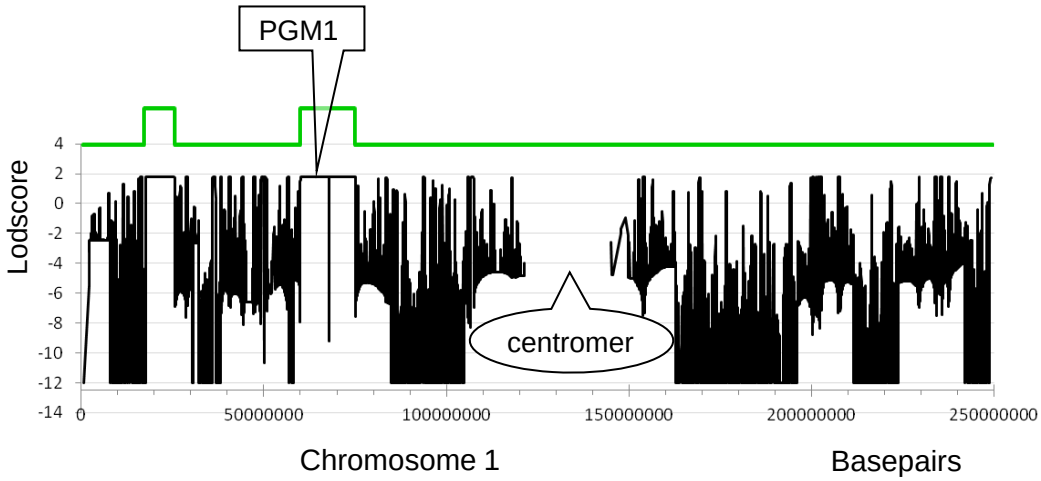

Figure S5. Pedigree of Family 1 and Homozygosity Mapping. (continued on next page)

A. A male sib pair (individuals 1.1 and 1.2; Table S1) affected by the mixed type CDG-disease was used for definition of a candidate region by homozygosity mapping. Grey symbols: no DNA available. Black shading of symbols shows segregation of the mutation identified in *PGM1*: full filled symbols: homozygotes, half-filled symbols: heterozygotes.

B. Mapping result shown for chromosome 1. Details of the procedure are given in supplementary methods. The maximal lod score was 1.8057. Elevated green line indicates homozygous candidate regions.

C. Mapping results of all other autosomal chromosomes with homozygous regions > 1 Mb.

Mapping and next generation sequencing led to the identification of *PGM1* as the primary candidate with a point mutation in this gene. The parents and additional unaffected sibs were used to demonstrate segregation of this mutation in the pedigree leading to disease in the homozygous mutation carriers only (black shading in panel A).

Figure S5 - continued: Pedigree of Family 1 and Homozygosity Mapping. Panel C

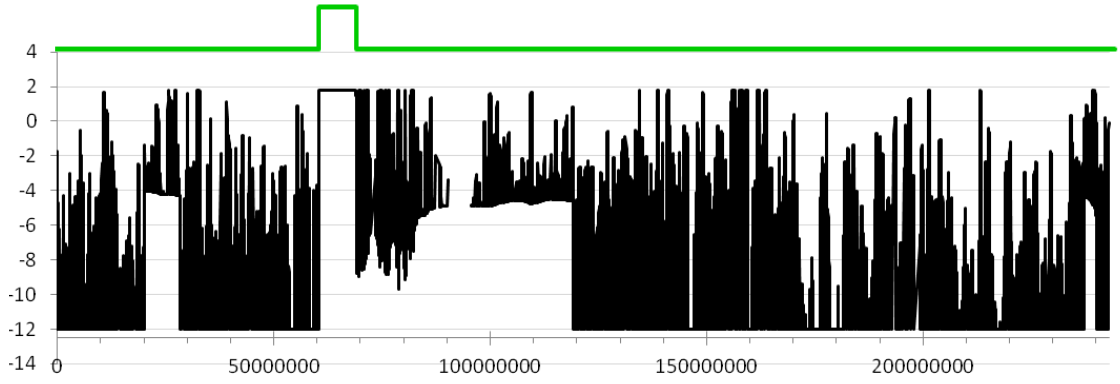

Chromosome 2, Lodscore/ Basepairs

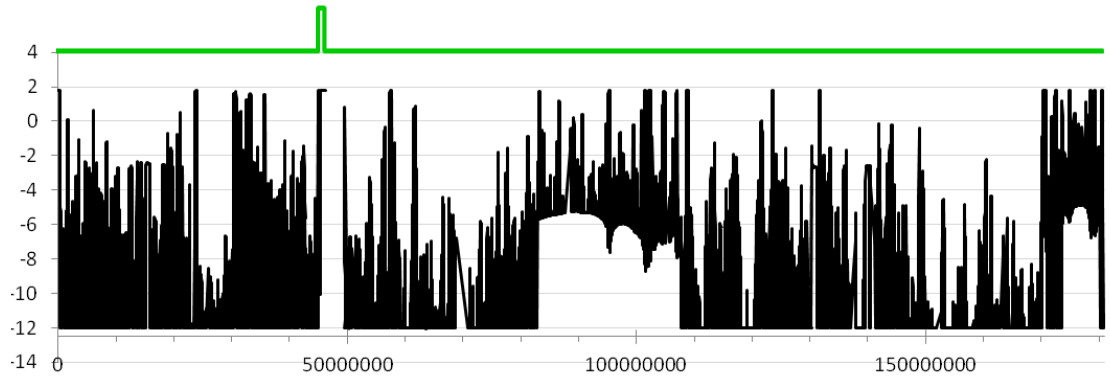

Chromosome 5, Lodscore/ Basepairs

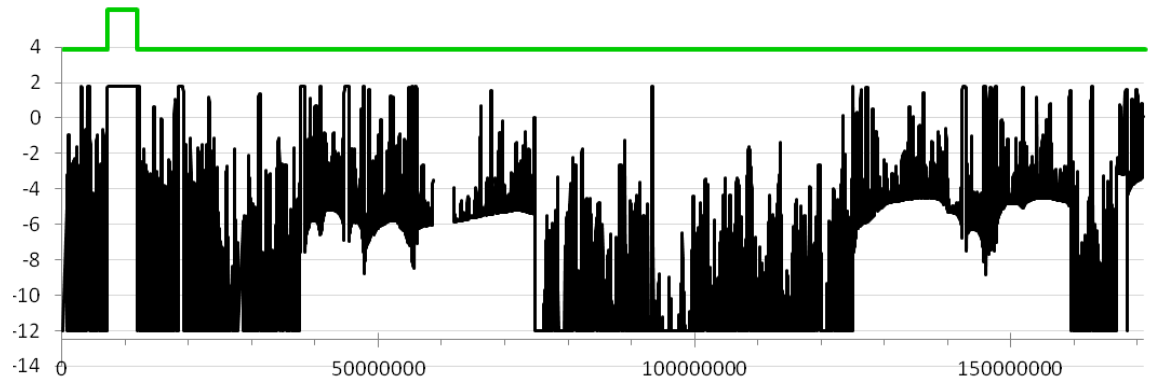

Chromosome 6, Lodscore/ Basepairs

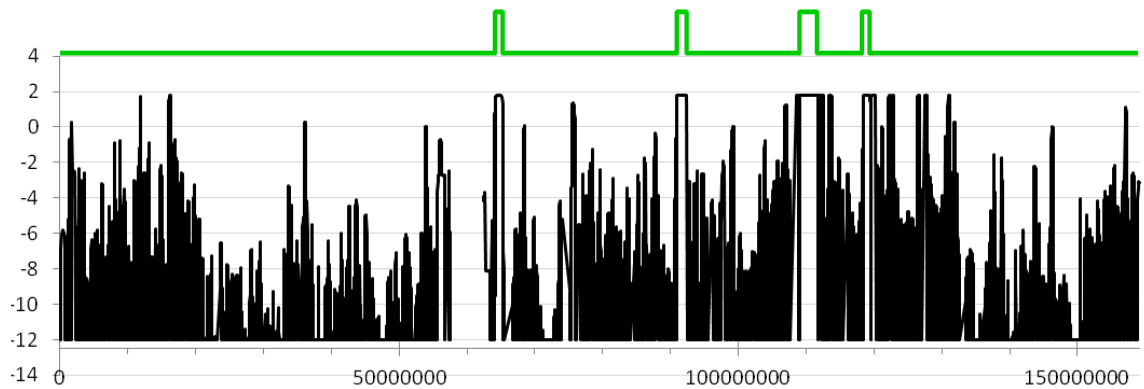

Chromosome 7, Lodscore/ Basepairs

Figure S5 - continued: Pedigree of Family 1 and Homozygosity Mapping. Panel C

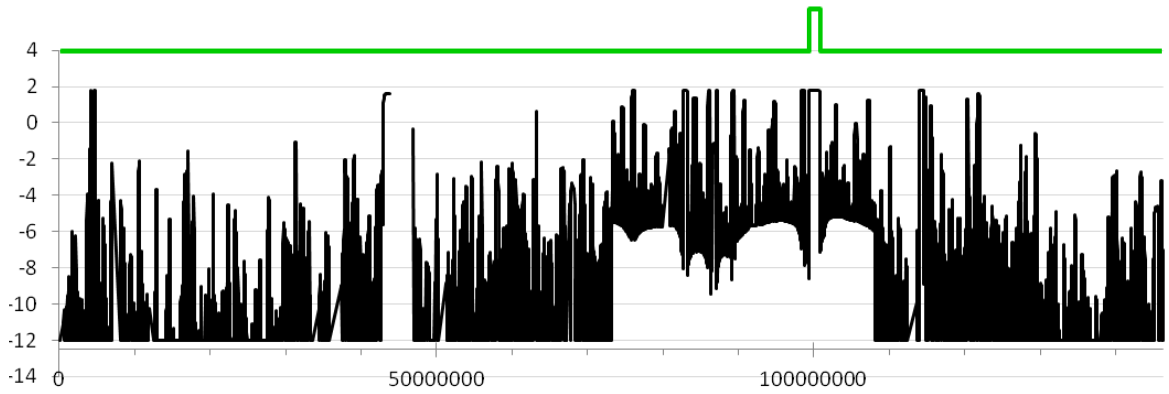

Chromosome 8, Lodscore/ Basepairs

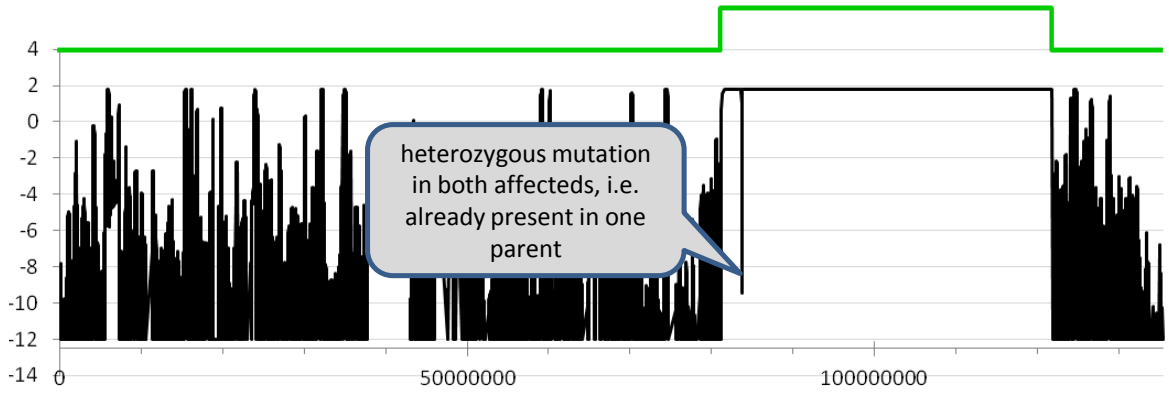

Chromosome 10, Lodscore/ Basepairs

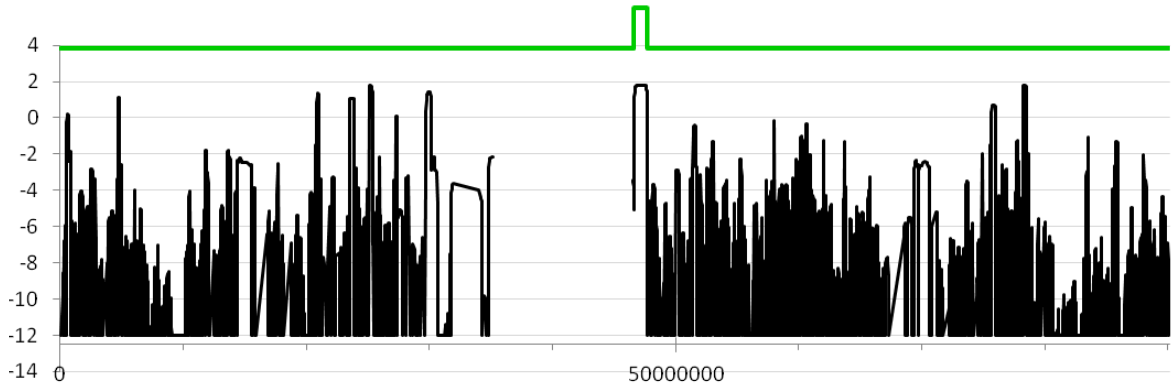

Chromosome 16, Lodscore/ Basepairs

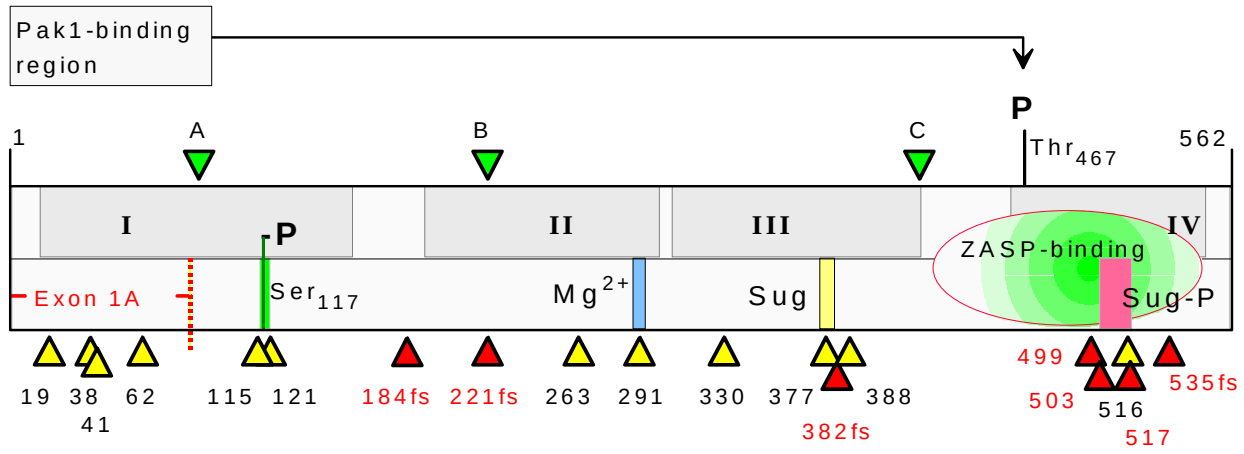

Figure S6. Details on PGM1 Structure and Mutations.

Schematic drawing of PGM1 with four domains[30,31] that are shown as grey shadowing (limits from Arimura[29]). Structural features as published are: PAK1 binding region < pos. 90[32]; catalytic site phospho-serine[33] (pos. 117, conserved amino acids 116-120; numbering based on UniProtKB/ Swiss-Prot:P00949); Mg^{2+}-binding site (DGDGDR, pos. 288-93)[31]; Sug (CGEESFG, pos. 374-80)[31]: binding of the sugar body; Sug-P (RLSGTGSAGATIRLY, pos. 503-517): binding of the phosphate of the incoming phosphosugar[31]; ZASP (pos. 427-562, most likely 489-562[29]): region binding of PGM1 to Zasp protein; Thr467; threonine phosphorylated by PAK1 leading to increased PGM1 activity.[32,34] Three common missense variants are indicated as A (rs855314, I88V), B (rs1126728, R221C), and C (rs11208257, Y420H) above the ribbon with green triangles. Variants B and C change the charge of the protein and explain the common IEF-variants of PGM1[35], used for decades in paternity testing. PGM1-deficiency mutations are indicated below the ribbon with yellow (missense) or red (stop) triangles and the (first affected) amino acid position (details of mutations s. Table S1). In fast muscle a rare alternative transcript has been described using an alternative exon 1, so that all mutations of the regular exon 1A will be excluded.

Frameshift mutations F184Sfs*9, R221Vfs*13 are sufficiently described in Table S1. In cDNA of sibs 5.1/2, the mutation c.1145-222G>T creates a new splice donor site, causing use of a cryptic splice site 120 bp upstream as acceptor site. Thus, the mutated allele produces a mRNA containing an additional exon derived from intronic sequence (r.[1145-222g>u; 1144_1145ins1145-343_1145-224] with the additional sequence c.1145-343_1145-224: TTCTGCAGGCTG ... GAGAGTGAAGGG). This translates to G382Vfs*23 at protein level. In patient 12, the mutation 1600-523G>A (M535Pfs*60) creates a new splice acceptor site and in addition downstream a cryptic splice donor site within the normal intron is activated. Thus, also in this case an additional exon is generated with insertion of 149 bases in the mRNA: r.[1600-523g>a;1599_1600ins1600-521_1600-373] (GTCCCTCCCACA ... TCACTGCTCCAG). RNA of patient 8 for analysis of 1145-1G>C was not available.

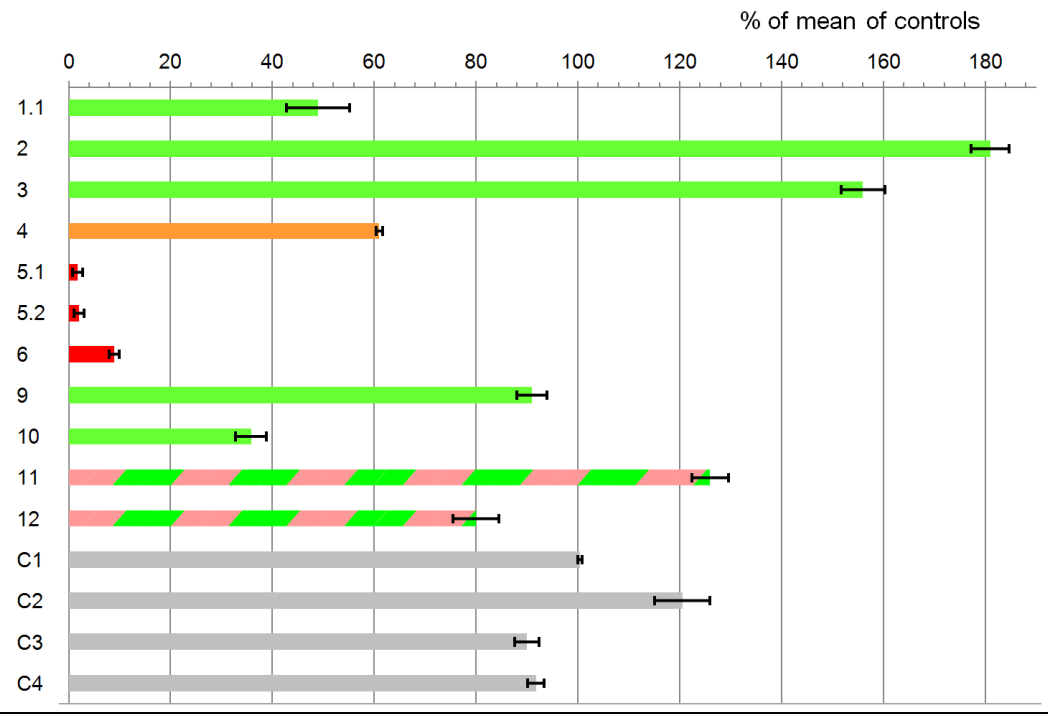

Figure S7. Real-Time PCR for Quantification of PGM1-mRNA in Fibroblasts.

We obtained either fibroblasts for cell culture, frozen fibroblast pellets for RNA-isolation, isolated RNA or cDNA from 11 patients and 4 controls. Numbers at the left are patient identifiers as in Table S1. C1-C4 are four different controls (grey bars). Results from patients with a homozygous stop codon leading to nonsense-mediated mRNA decay[36] are shown in red (5.1, 5.2, 6). The orange bar represents patient 4, a compound heterozygote having one nonsense allele expected to undergo nonsense-mediated decay. The light red/green hatching was used for compound heterozygotes (11, 12) having one nonsense allele, that is expected to be stable, since the position of the stop codon is predicted not to elicit nonsense-mediated mRNA-decay.[36] All other patients carrying missense variants are represented by green bars. To predict expected changes in mRNA-level from nonsense mutations, we determined the position of the different stop codons relative to the last splice junction. According to the rules and mechanisms reported in literature nonsense-mediated mRNA decay was expected only in homozygous patients 5.1, 5.2, and 6 as well as in the heterozygote 4, since only in these cases the stop codon was at least 50 bp before the last splice junction.[36] Note that mRNA of patient 6 showed some escape from nonsense-mediated decay (mRNA-level 8.9 % of controls).

The method is described above, section "Real-time PCR for quantification of PGM1 mRNA"

PGM1-mRNA levels show some variability that in part may be due to the various sources of cDNA analyzed. To check PGM1-levels in population we used data from a large scale study of mRNA-levels of about 39000 transcripts in 427 liver samples[37] that were available from Gene Expression Omnibus database entry GSE9588. Analysis demonstrated a calculated standard deviation of PGM1-levels of 54 % but an asymmetric distribution with a range from 45 to 240 % of mean PGM1-mRNA-level covering 95 % of samples. In addition these authors reported an association of a frequent SNP in the 3'UTR of PGM1 (rs4643, minor allele frequency 20 %) with PGM1 expression level (p = 1.01E-06). This SNP has also been reported to be associated with variability of the reduced glycosylation ("CDT", carbohydrate-deficient transferrin) that is observed as consequence of alcohol abuse.[38]

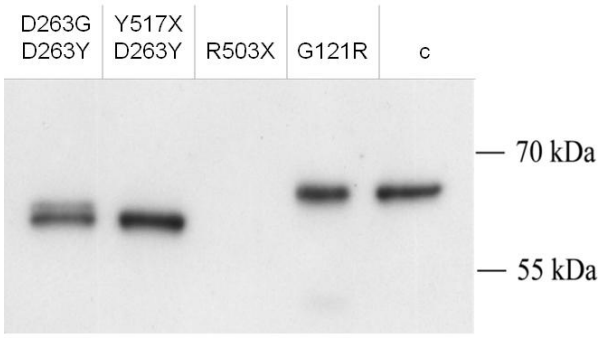

Figure S8. Western Blot of PGM1 from PGM1 Deficient Fibroblasts.

In 13 patients PGM1 protein was analyzed by Western blot. Often, no protein was visible as in the third lane (R530X-mutation, patient 6; for patient numbers see Table S1) or only very faint bands could be observed (not shown). The mutations D263Y and D263G show lower molecular masses (patient 3 in lane 1, patient 11 in lane 2). Analysis of the *PGM1* transcript revealed no truncations so that the nature of the apparent mass loss remains unclear but may be partial degradation of the protein.

Normal amount of regular sized protein was observed for G121R (lane 4, patient 7) and G291R (patient 9, not shown). Nevertheless PGM1 activity was close to background for G121R - this is likely due to an effect on the catalytic active center, with Ser-117 carrying the phosphate-group involved in the phosphoglucomutase reaction. G291[39] is located within a Mg^{2+} binding site indicated as blue bar in Fig. S6, see above, that in a 3-D-model of PGM1 is in close vicinity to the Ser-117-P and is involved in coordination of the phosphate and necessary for catalysis (DGDGDR, pos. 288-93).[31]

In summary, patients 3, 7, 9, and 11 showed some considerable protein signal, while 1.1, 1.2, 2, 4, 5.1, 5.2, 6, 10, 12 showed no or only very faint signal. From patients 8, 13.1/2, 14, 15, 16, carrying additional missense mutations T19A, D62H, T115A and E388K, no protein samples were available for analysis.

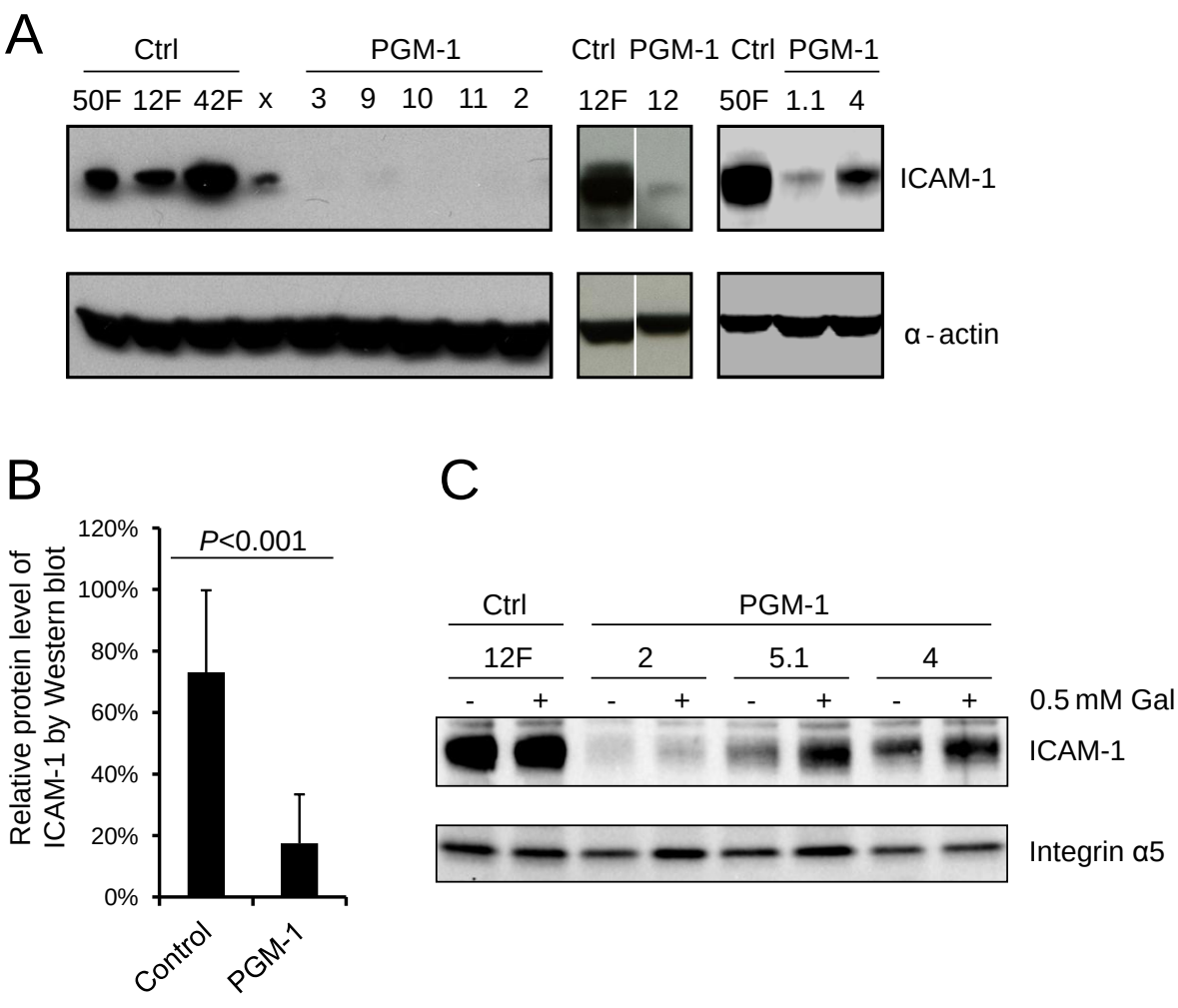

Figure S9. Western Blotting of Fibroblast ICAM-1.

ICAM-1 has 8 occupied N-glycosylation sites[40] and is highly suitable to check cultured cells for glycosylation efficiency, since ICAM-1 on Western blots is strongly diminished due to underglycosylation.[10] The figure demonstrates that ICAM-1 is a suitable measure for glycosylation efficiency also in PGM1-deficient cells (A and B). Galactose supplementation could partially restore the ICAM-1 expression in PGM-1 patients' cells (increase of 1.5-fold up to 8-fold, panel C). PGM-1 sample numbers correspond to those of Table S1.

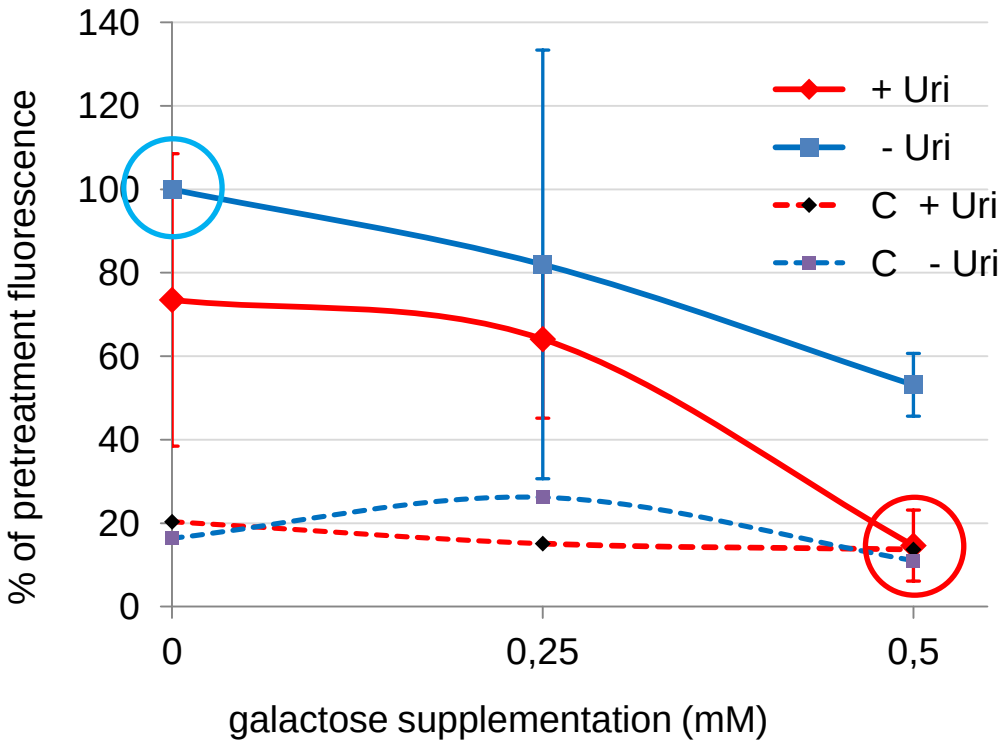

Figure S10. Galactose and Uridine Supplementation in Patients' Fibroblasts

ER-retained GFP, engineered to contain an N-glycosylation site that destroys fluorescence when it is glycosylated (Glyc-ER-GFP)[11], was transfected into PGM1-deficient fibroblasts as a marker for impaired glycosylation. Testing different conditions in cell culture (see supplementary method: Assay for cellular glycosylation efficiency using modified GFP) we found that supplementation of 3 different patient cell lines with 0.5 mM galactose and 100 µM uridine reduced fluorescence of Glyc-ER-GFP to 15 % (+-7 % (SD); red circle) of the individual pretreatment fluorescence (100 %: blue circle). Normal control cells almost completely glycosylate the GFP and background fluorescence is typically about 10-20% of untreated values from patient cells (broken lines). This means that combined optimal supplementation with galactose and uridine achieved fully normal glycosylation in patient cells - see overlay of controls and patient data points in the red circle.

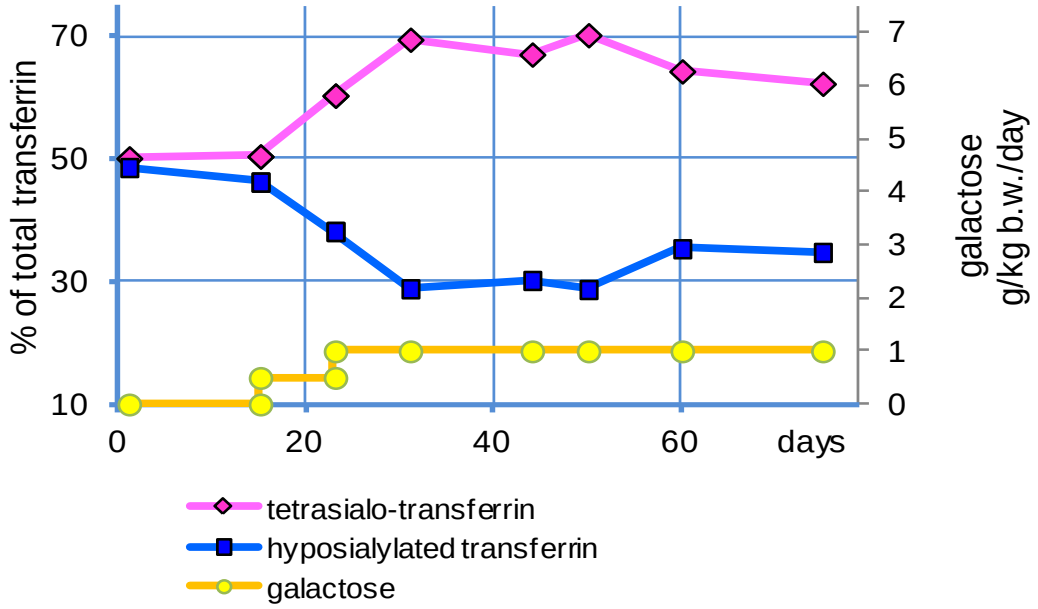

Figure S11. Dietary Effect of Galactose on Transferrin Glycosylation

Patient 1.1 started to take galactose at a daily dose of 0.5 g per kg b.w. divided into 3 portions at day 15, doubled after one week. Effect on transferrin isoforms was quantitated by HPLC (tetrasialo and hyposialylated forms). Within a few weeks tetrasialo-transferrin had increased from 50 up to 70% with a corresponding decrease of the hyposialylated isoforms.

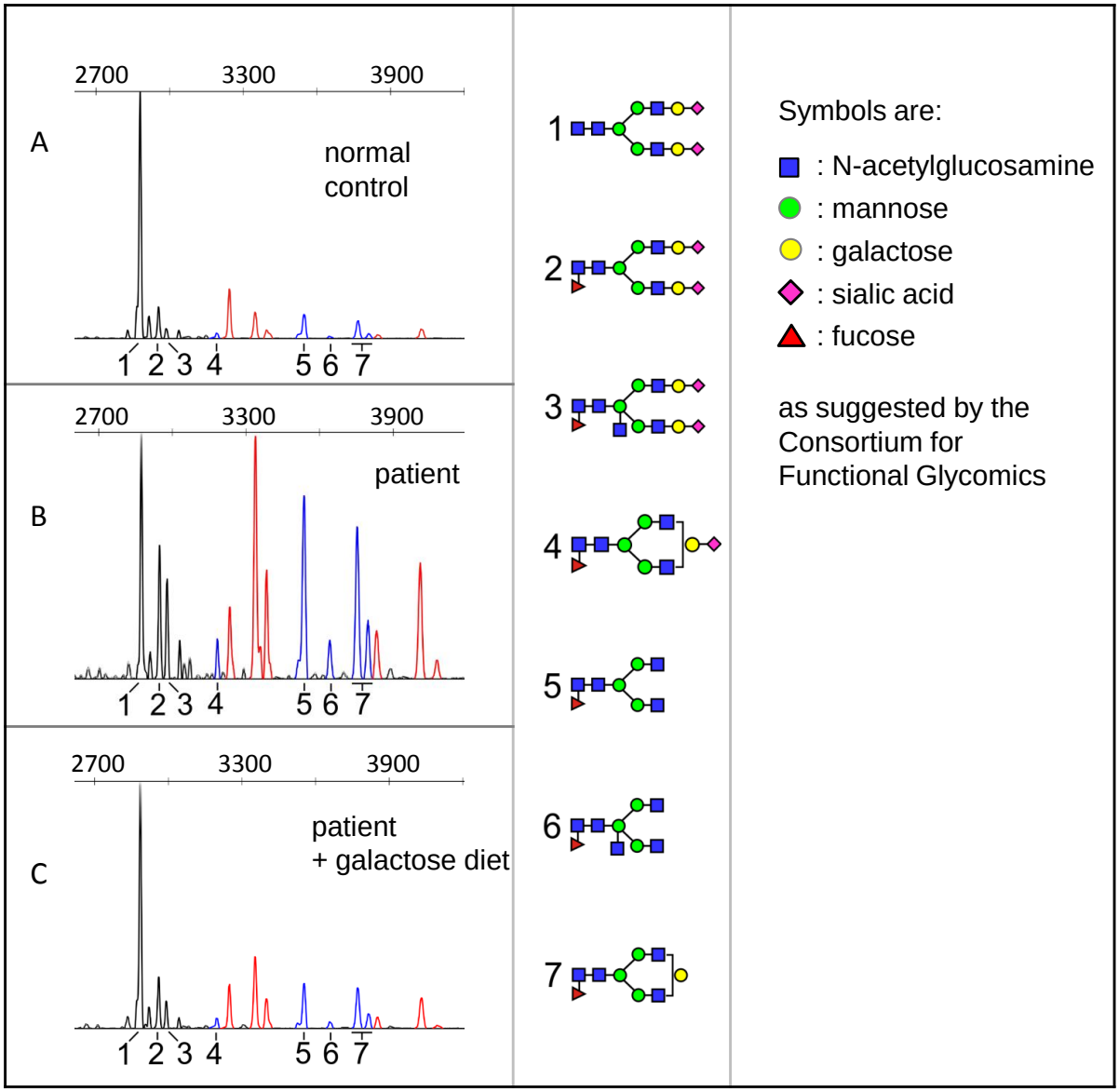

Figure S12. Dietary Effects of Galactose on total Serum Glycome.

Panels A-C show the analysis of total serum N-glycome before and during galactose supplementation. The glycans are cut from the proteins and analyzed by capillary electrophoresis on a standard ABI-3130 capillary sequencer. The sample processing has been described completely elsewhere[41], with the only modification that samples were not desialylated. Panel A shows a normal control, panel B a patient before galactose supplementation, C same patient during galactose supplementation. Glycans lacking one or more sialic acid residues only, but missing no galactose, are depicted in red, those lacking also galactose in blue. Peaks 1-3 are fully sialylated glycans. To show the effect of missing galactose all blue peaks were also numbered and detailed structures are given in the right panel. The figure shows that galactose supplementation normalizes to a large extent the glycosylation of total serum glycoproteins (not only transferrin).

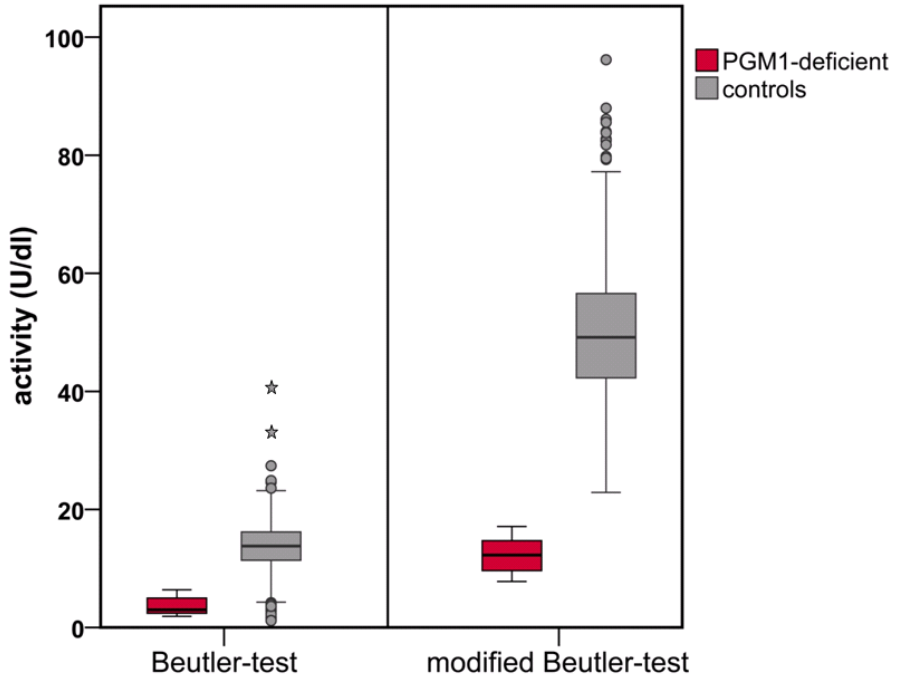

Figure S13. Performance of Guthrie Screening Assay for PGM1-Deficiency

Dried blood spots of the GALT kit calibrators and controls, as well as samples from 8 patients with PGM deficiency and anonymised DBS from 2017 healthy newborns were analyzed. Using the unmodified Beutler test (box-plot left panel) as measure of PGM1 activity, intra- and interassay variation was less than 10% for PGM activities between 3 U/dl to 40 U/dl. GALT activity from the 8 patients with PGM deficiency was significantly lower than in the healthy newborns ($p = 0.014$), however, there was significant overlap (extreme values in controls indicated by asterisks). The addition of PGM from rabbit heart restored the GALT-activity in the DBS of PGM-deficient patients to normal values (Table S4).

When the Beutler test was modified, the difference between PGM activity in DBS from PGM-deficient patients and healthy newborns was highly significant ($p < 0.001$) with a clear discrimination between the two groups (right panel; Table S4). Using a preliminary cut-off at 0.1%, all PGM1-deficient patients were recognized (sensitivity 100%, specificity > 99.9%). A pilot study will be necessary to determine true and false positive rate in the population in order to determine the positive predictive value of the assay.

In erythrocytes 50 % of PGM-activity is contributed by PGM2. However, this should not interfere with our assay results, since PGM2 has PGM activity only at high concentrations of its cofactor glucose-1,6-bisphosphate (Glc-1,6-BP; in erythrocytes about 590 µM), while below 190 µM PGM2 has mainly phosphopentose mutase activity.[19] In our assay volume of 100 µl there is about 1.5 µl volume equivalent to erythrocytes. Thus, Glc-1,6-BP is diluted to about 10 µM. A small contribution of up to 7 µM may also come from contamination of the substrate glucose-1-phosphate by glucose-1,6-diphosphate (Sigma No. G6875, 0.01-0.2%).

Handling of Guthrie spots is the same as in galactosemia screening. If necessary samples can be stored at -18°C for months without any detectable change in GALT or PGM1-activity.

SUPPLEMENTARY TABLES

Table S1. Biochemical and Clinical Features in PGM1 Deficiency

Patient	1.1	1.2	2	3	4	5.1	5.2	6	7	8	9	10	11	12	13.1	13.2	14	15	16
Trait																			
Current age/sex	12/m	17/m	19/f	33/m	19/m	26/m	20/f	16/f	8/m	43/m	23/f	9/f	11/m	9/m	5/m	6/m	10/m	3/f	30/f
PGM1 defect ✝ cDNA	1547T>C		988G>C 1129G>A	787G>T 788A>G	122A>G 1495C>T	1145-222G>T		1507C>T	361G>C	343A>G 1145-1G>C	122A>G 871G>A	112A>T	787G>T 1551C>A	55A>G 1600-523G>A	184G>C		1162G>A 1547T>C	551delT	787G>T 661delC
protein	L516P		G330R E377K	D263Y D263G	Q41R R499X	G382Vfs*23		R503X	G121R	T115A Splice	Q41R G291R	N38Y	D263Y Y517X	T19A M535Pfs*60	D62H		E388K L516P	F184Sfs*9	D263Y R221Vfs*13
activity **$** (% of controls)	4.4	NA	1.3	2.4	2.5	2.2	2.8	7.7	6.6	1.2	12	3.1	2.8	3.3	2.1	2.8	1.2	NA	0.3
Head																			
bifid uvula (BU) cleft palate (CP) Pierre-Robin sequence (PRS)	CP,BU	CP, BU	CP,BU & PRS	BU	-	CP, BU	CP, BU & PRS	CP, BU & PRS	CP, BU & PRS	-	-	CP, BU & PRS	CP, BU & PRS	CP, BU & PRS	CP, BU & PRS	CP, BU & PRS	CP, BU	CP, BU	CP, BU
Heart																			
dilated cardio-myopathy	-	-	severe FS 5%	-	-	LV slightly enlarged	severe FS 7%	severe FS 5%	severe FS 5%	-	-	-	-	-	-	-	severe FS <10%	-	-
cardiac arrest	-	-	-	yes, resuscitated	-	-	yes, resuscitated	-	yes, deceased	-	-	-	-	-	-	-	yes, deceased	-	-
Skeletal muscle	exercise intol.	exercise intol.	exercise intol.	NA	-	exercise intol.	exercise intol.	-	muscle weakness	exercise intol.	-	-	muscle weakness	exercise intol.	-	-	-	-	exercise intol.
Max. CK (U/l)	789	380	50 000	NA	<300	10 000	7942	10 000	250	10 000	<300	3000	<300	2000	200	200	NA	NA	10 000
Rhabdomyolysis (R) Malignant hyperthermia (M)	-	-	R, M	-	-	R	-	M, R	-	R	-	-	-	-	-	-	-	-	R
Liver																			
AST, ALT ‡ increased	Yes	Yes	Yes	Yes	Yes	Yes	Yes	Yes	Yes	Yes	Yes	Yes	Yes	Yes	Yes	Yes	Yes	Yes	Yes
biopsy results ¢	steatosis mild fibrosis	-	increased glycogen, steatosis	-	cholestasis, fibrosis, steatosis	-	-	increased glycogen, steatosis	-	-	cholestasis, steatosis	-	-	-	-	-	-	-	-
Lowest blood glucose (mM)	2.6	2.8	1.0	1.9	1.8	2.8	3.2	1.8	2.6	4.2	1.6	<2.7	2.4	1.4	2.1	2.4	2.6	2.4	3.6
Growth ¥ *(height percentile: "pc")*	<3 pc	3 pc	<5 pc	< 3 pc	50 pc	3 pc	<3 pc	<3 pc	<3 pc	90 pc	75 pc	10-15 pc	<5 pc	<5 pc	<5 pc	<5 pc	<5 pc	<3 pc	<3 pc
Endocrine																			
LH (ref. 0.6 - 16 U/L)																			
before galactose	-	-	0,6	-	-	-	-	0.5	-	-	-	-	-	-	-	-	-	-	-
after galactose #	-	-	3.1-3.5	-	-	-	-	4.0-6.2	-	-	-	-	-	-	-	-	-	-	-
FSH (ref. 3.3 - 19 U/L)																			
before galactose	-	-	2	-	-	-	-	2.9	-	-	-	-	-	-	-	-	-	-	-
after galactose	-	-	5.4-6.5	-	-	-	-	4.9-10	-	-	-	-	-	-	-	-	-	-	-

Table S1. Biochemical and Clinical Features in PGM1 Deficiency.
Families 1, 5, and 13 each included an affected sib pair (1.1, 1.2 etc.). ✝ PGM1 defects: Mutations were numbered based on NM_002633.2 (cDNA) and NG_016966.1 (genomic DNA). Where biological parents were available, both carried an allele of their affected children (7 and 13.1/13.2 were adopted, biological parents not available). **$** PGM1 activity was assayed in fibroblasts or leukocytes or from muscle biopsies (patients 8 and 16) and expressed as percentage of the mean control. Effects of mutations on function, structure and expression of mRNA, and on protein levels are detailed in the Figures S6, S7, S8. ‡ ASAT and ALAT levels were mildly elevated from just above normal to 500 U/l (measured in the absence of rhabdomyolysis). ¢ Liver biopsies were evaluated by light microsopy and electron microscopy (Fig. S3). ¥ Growth: All but one of patients with a split uvula also had short stature (< 5th percentile in 15) but all three with a normal uvula had also normal height. # Hormones after galactose: measurements between month 2 - 11 after starting galactose supplementation. FS, fractional shortening (patients' lowest ever measured values); CK, creatine kinase; AST, aspartate aminotransferase; ALT, alanine aminotransferase; LH, luteinizing hormone; FSH, follicle-stimulating hormone; NA, data not available.

Table S2. PCR Primers and Conditions.

For sequencing reactions, each forward primer was tagged at the 5´site with the universal primer TGT AAA ACG ACG GCC AGT ("F-"). Each reverse primer was tagged at the 5´site with CAG GAA ACA GCT ATG ACC ("R-"). PCR-conditions were: initial denaturation 5 min. 94°C, cycling 35 x (1 min. 94°C, 1 min. at annealing temperature given in tables below, 1.5 min. 72°C), 10 min. 72°C.

Table S2.1 Genomic DNA

Exon	Primer sequence (5´to 3´)	PCR conditions (annealing temperature, +/-Q: Q-solution from Qiagen, Hilden, Germany)
Ex1 variant 1	F-GTC CCT TTA AGG AGG AGG GC R-GAG TCA GGC GAG CAG GTC TG	67°C; +Q
Ex1 variant 2	F-CTT TGT GTG TGG GTG CGA GT R-CTT AAG ACC GGG AGT GTG CT	67°C; +Q
Ex2	F-CCT TAC AGT GCA CAC AG R-GAA GCA AAG AGC ACC TCC CT	65°C; +Q
Ex3	F-CCA TGC GCA AAT CTT CC R-TCA TGC AGC TGA TCC CTG GC	65°C; +Q
Ex4	F-ATC CCC TGT GTG CCT CAT CC R-CTT ACC ACG AGG AGT GTC TC	67°C; -Q
Ex5	F-CTC CAC TAG TCC CTG AAC AC R-GCA TCT AGA ACT CAC CCA GC	67°C; -Q
Ex6	F-GCC TTC GGC CCA ATG GTA CT R-GAG AGG GGC ATT GAA TCC AG	67°C; -Q
Ex7	F-TTC TTC TTC CGC CTT CTC TG R-TCC CTG CAG ACT CAA TGA CC	67°C; -Q
Ex8	F-CAG CAA GGG GGA ACT TTG TC R-CAT GTC CAC CCA ATG GAC AC	67°C; -Q
Ex9	F-GTT CCA TCC CCA GTG ACT GA R-GTG GGA CAG CAG AAA ACC AG	67°C; -Q
Ex10	F-CAC CCA GCA TCA CTG AGG TC R-CAG GCT TGA CCT CCT GGG CT	65°C; +Q
Ex11	F-GCA GAG GAA GAT GTC AGG AG R-CAG CTC CCA AGG GCA TCT TG	65°C; -Q

Table S2.2. **cDNA**

I	F-CCT TTC CCC TCC CGC CGG AC R-GCA CCG AGT TCT TCA CAG AG	65°C; +Q
II	F-CTG GGC CAA ACC GAC TGA AG R-TGG ATG GGT CCG GGG GTG	65°C; +Q

Table S3. Glycogen Content in Patient Fibroblasts

		% of cells with glycogen
5.5 mM Glucose	Control1	17%
	Control2	16%
	PGM1-6	<1%
	PGM1-7	<1%
5.5 mM Galactose	Control 1	2%
	Control 2	4%
	PGM1-6	<1%
	PGM1-7	<1%

Fibroblasts were prepared for evaluation of glycogen by electron microscopy as described above. The presence of glycogen in control and patient fibroblasts cultured in the presence of either glucose or galactose was assessed by electron microscopy. Cells (of 115-160 total) with small darkly staining aggregates of glycogen were counted as positive. Aggregates are typically more common in glycogen storage diseases (picture for hepatocytes s. Fig. S3, panel C, D).

At a first glance these results might give the impression that glycogen is even reduced in PGM1 deficient patients. However, cells in culture contain glycogen of different quality. The glycogen counted by electron microscopy (this table) has stronger staining aggregate grains only. It should be noted that the values are % of cells containing any such aggregates, i.e. more than 80 % of control cells and almost all PGM1-cells didn't show such aggregates, therefore the majority of the normal cells were comparable with PGM1-cells. Glycogen measurement by a biochemical method measured all glycogen instead, including diffuse glycogen, not gathered in aggregates, revealing that the total glycogen amount is not significantly different - only the number of cells with stronger staining aggregates seems in microscopy somewhat lower in the patients. Since this type of aggregates is significantly increased in patients with glycogen storage diseases, it was checked here.

Table S4. **Range of GALT-, PGM-, and G6PDH-Activities in 8 Patients with PGM1-Deficiency and in Healthy Newborns.**

Whereas GALT and G6PDH do not show clear discrimination between PGM1-deficient patients and controls, our modified assay shows highly significant differences of PGM activity in patients and controls. Design of the assay is described in Fig. S2. The addition of PGM from rabbit heart restored the GALT-activity in the DBS of PGM-deficient patients to normal values.

	GALT (U/dL)	GALT (U/dL) + PGM *	PGM (U/dL)	G6PDH (U/dL)
PGM def. (n=8)	1.9 – 6.5	6.4 – 17.4	7.8 – 17.1	139.4 – 331.2
Controls	3.4 – 40.7 (n = 2017) (median = 13.9)	11.9 – 15.3 (n = 4)	17.5 – 96.2 (n = 2017) (median = 49.3)	46.1 – 559.5 (n = 1737) (median = 292.0)

* = PGM from rabbit muscle was added to the DBS in the GALT assay.

References:

1. Abecasis GR, Cherny SS, Cookson WO, Cardon LR. Merlin--rapid analysis of dense genetic maps using sparse gene flow trees. Nat Genet 2002;30:97-101.
2. Roach JC, Glusman G, Smit AF, et al. Analysis of genetic inheritance in a family quartet by whole-genome sequencing. Science 2010;328:636-9.
3. Nachman MW, Crowell SL. Estimate of the mutation rate per nucleotide in humans. Genetics 2000;156:297-304.
4. Timal S, Hoischen A, Lehle L, et al. Gene identification in the Congenital Disorders of Glycosylation type I by whole-exome sequencing. Hum Mol Genet 2012;21:4151-61.
5. Hoischen A, van Bon BW, Rodriguez-Santiago B, et al. De novo nonsense mutations in ASXL1 cause Bohring-Opitz syndrome. Nat Genet 2011;43:729-31.
6. Rozen S, Skaletzky HJ. Primer3 on the WWW for general users and for biologist programmers. In: Krawetz S, S. M, eds. Bioinformatics Methods and Protocols: Methods in Molecular Biology. Totowa, NJ: Humana Press; 2000:365-86.
7. Lowry OH, Rosebrough NJ, Farr AL, Randall RJ. Protein measurement with the Folin phenol reagent. J Biol Chem 1951;193:265-75.
8. Babovic-Vuksanovic D, O'Brien JF. Laboratory diagnosis of congenital disorders of glycosylation type I by analysis of transferrin glycoforms. Mol Diagn Ther 2007;11:303-11.
9. Wada Y, Tajiri M, Yoshida S. Hydrophilic affinity isolation and MALDI multiple-stage tandem mass spectrometry of glycopeptides for glycoproteomics. Anal Chem 2004;76:6560-5.
10. He P, Ng BG, Losfeld ME, Zhu W, Freeze HH. Identification of intercellular cell adhesion molecule 1 (ICAM-1) as a hypo-glycosylation marker in congenital disorders of glycosylation cells. J Biol Chem 2012.
11. Losfeld ME, Soncin F, Ng BG, K. S, Freeze HH. A sensitive Green Fluorescent Protein biomarker of N-glycosylation site occupancy. FASEB J 2012;in press.
12. Rabina J, Maki M, Savilahti EM, Jarvinen N, Penttila L, Renkonen R. Analysis of nucleotide sugars from cell lysates by ion-pair solid-phase extraction and reversed-phase high-performance liquid chromatography. Glycoconj J 2001;18:799-805.
13. Nakajima K, Kitazume S, Angata T, et al. Simultaneous determination of nucleotide sugars with ion-pair reversed-phase HPLC. Glycobiology 2010;20:865-71.
14. Shin YS. Galactose metabolites and disorders of galactose metabolism. In: Hommes FA, ed. Techniques in diagnostic human biochemical genetics. New York: Wiley-Liss; 1991:267-83.
15. Donthi RV, Epstein PN. Altering and analyzing glucose metabolism in perfused hearts of transgenic mice. Methods Mol Med 2007;139:151-61.
16. Passonneau JV, Lauderdale VR. A comparison of three methods of glycogen measurement in tissues. Anal Biochem 1974;60:405-12.
17. Sickmann HM, Schousboe A, Fosgerau K, Waagepetersen HS. Compartmentation of lactate originating from glycogen and glucose in cultured astrocytes. Neurochem Res 2005;30:1295-304.
18. McAlpine PJ, Hopkinson DA, Harris H. The relative activities attributable to the three phosphoglucomutase loci (PGM1, PGM2, PGM3) in human tissues. Ann Hum Genet 1970;34:169-75.

19. Quick CB, Fisher RA, Harris H. A kinetic study of the isozymes determined by the three human phosphoglucomutase loci PGM1, PGM2, and PGM3. Eur J Biochem 1974;42:511-7.
20. Maliekal P, Sokolova T, Vertommen D, Veiga-da-Cunha M, Van Schaftingen E. Molecular identification of mammalian phosphopentomutase and glucose-1,6-bisphosphate synthase, two members of the alpha-D-phosphohexomutase family. J Biol Chem 2007;282:31844-51.
21. Pirard M, Achouri Y, Collet JF, Schollen E, Matthijs G, Van Schaftingen E. Kinetic properties and tissular distribution of mammalian phosphomannomutase isozymes. Biochem J 1999;339 (Pt 1):201-7.
22. Huhtaniemi IT. Polymorphism of gonadotropin action: clinical implications. Asian J Androl 2000;2:241-6.
23. Sairam MR, Fleshner P. Inhibition of hormone-induced cyclic AMP production and steroidogenesis in interstitial cells by deglycosylated lutropin. Mol Cell Endocrinol 1981;22:41-54.
24. Galway AB, Hsueh AJ, Keene JL, Yamoto M, Fauser BC, Boime I. In vitro and in vivo bioactivity of recombinant human follicle-stimulating hormone and partially deglycosylated variants secreted by transfected eukaryotic cell lines. Endocrinology 1990;127:93-100.
25. Miller BS, Khosravi MJ, Patterson MC, Conover CA. IGF system in children with congenital disorders of glycosylation. Clin Endocrinol (Oxf) 2009;70:892-7.
26. Niehues R, Hasilik M, Alton G, et al. Carbohydrate-deficient glycoprotein syndrome type Ib. Phosphomannose isomerase deficiency and mannose therapy. J Clin Invest 1998;101:1414-20.
27. Carlberg M, Larsson O. Stimulatory effect of PDGF on HMG-CoA reductase activity and N-linked glycosylation contributes to increased expression of IGF-1 receptors in human fibroblasts. Exp Cell Res 1996;223:142-8.
28. Vatta M, Mohapatra B, Jimenez S, et al. Mutations in Cypher/ZASP in patients with dilated cardiomyopathy and left ventricular non-compaction. J Am Coll Cardiol 2003;42:2014-27.
29. Arimura T, Inagaki N, Hayashi T, et al. Impaired binding of ZASP/Cypher with phosphoglucomutase 1 is associated with dilated cardiomyopathy. Cardiovasc Res 2009;83:80-8.
30. Dai JB, Liu Y, Ray WJ, Jr., Konno M. The crystal structure of muscle phosphoglucomutase refined at 2.7-angstrom resolution. J Biol Chem 1992;267:6322-37.
31. Shackelford GS, Regni CA, Beamer LJ. Evolutionary trace analysis of the alpha-D-phosphohexomutase superfamily. Protein Sci 2004;13:2130-8.
32. Gururaj A, Barnes CJ, Vadlamudi RK, Kumar R. Regulation of phosphoglucomutase 1 phosphorylation and activity by a signaling kinase. Oncogene 2004;23:8118-27.
33. Milstein C, Sanger F. An amino acid sequence in the active centre of phosphoglucomutase. Biochem J 1961;79:456-69.
34. Hindle AG, Karimpour-Fard A, Epperson LE, Hunter LE, Martin SL. Skeletal muscle proteomics: carbohydrate metabolism oscillates with seasonal and torpor-arousal physiology of hibernation. Am J Physiol Regul Integr Comp Physiol 2011;301:R1440-52.
35. March RE, Putt W, Hollyoake M, et al. The classical human phosphoglucomutase (PGM1) isozyme polymorphism is generated by intragenic recombination. Proc Natl Acad Sci U S A 1993;90:10730-3.

36. Maquat LE. Nonsense-mediated mRNA decay in mammals. J Cell Sci 2005;118:1773-6.
37. Schadt EE, Molony C, Chudin E, et al. Mapping the genetic architecture of gene expression in human liver. PLoS Biol 2008;6:e107.
38. Kutalik Z, Benyamin B, Bergmann S, et al. Genome-wide association study identifies two loci strongly affecting transferrin glycosylation. Hum Mol Genet 2011;20:3710-7.
39. Perez B, Medrano C, Ecay MJ, et al. A novel congenital disorder of glycosylation type without central nervous system involvement caused by mutations in the phosphoglucomutase 1 gene. J Inherit Metab Dis 2012.
40. Bloom JW, Madanat MS, Ray MK. Cell line and site specific comparative analysis of the N-linked oligosaccharides on human ICAM-1des454-532 by electrospray ionization mass spectrometry. Biochemistry 1996;35:1856-64.
41. Vanderschaeghe D, Laroy W, Sablon E, et al. GlycoFibroTest is a highly performant liver fibrosis biomarker derived from DNA sequencer-based serum protein glycomics. Mol Cell Proteomics 2009;8:986-94.